

# Transient Metastability and Selective Decay for the Coherent Zonal Structures in Plasma Edge Turbulence

Di Qi <sup>a</sup> and Andrew J. Majda <sup>a</sup>

August 22, 2018

<sup>a</sup> Department of Mathematics and Center for Atmosphere and Ocean Science, Courant Institute of Mathematical Sciences, New York University, New York, NY 10012

## Abstract

The emergence of persistent coherent zonal structures is studied in the freely decay plasma flows. The plasma edge turbulence in the magnetic-fusion devices can be described qualitatively by the modified Hasegawa-Mima (MHM) model, which is shown to create enhanced zonal flows and more physically relevant features compared with the original Charney-Hasegawa-Mima (CHM) model. We analyze the generation and stability of the zonal state in the MHM model following the strategy for showing selective decay in the CHM model. The selective decay and metastable states are defined as critical points of the enstrophy at constant energy. The critical points are first shown to be invariant solutions to the MHM equation with a special emphasis on the zonal modes. Further, it is found that any initial states will converge to some critical point solution at long time limit with proper dissipation forms, while the zonal states are the only stable ones. Thus the decay process of the solutions can be characterized by the transient visits to several metastable states and then the final convergence to a purely zonal state. The selective decay and metastability properties are confirmed by numerical simulations with various distinct initial structures.

## 1 Introduction

The large-scale coherent structures and zonal flows are important and universally observed phenomena found in various experiments and simulations with different degrees of complexity, for example, in the mesoscale motions of the atmosphere and ocean [13, 22, 17, 21] and in the toroidally magnetically confined plasmas [1, 7, 2, 4]. In particular, the generation of zonal flows in the edge of magnetic confinement fusion has the crucial role in regulating the drift wave turbulence and withholding the disastrous particle transport towards the boundary regime [1, 2, 11, 18]. For qualitative understanding about the physics in the energy-conserving nonlinear dynamics and the formation of zonal jets, the Charney-Hasegawa-Mima (CHM) model (also known as the quasi-geostrophic model) is used to describe both the Rossby wave turbulence in geophysical turbulence [17] and the drift wave turbulence in plasma edge regimes [6]. In plasma physics, the equation provides a simple envelope formulation in describing the essential physics in drift wave – zonal flow nonlinear interactions in the tokamak edge turbulence. The flows are formulated on a projected two-dimensional domain in the perpendicular direction to the ambient magnetic field, where the three-dimensional magnetic surfaces are embedded.

A modified Hasegawa-Mima (MHM) model [4, 1] is introduced later as a more physically relevant formulation for the plasma flows. The MHM model takes into account the suppression of the magnetic-surface-averaged electron density response. The model modification gains the physically consistent property of Galilean invariance under poloidal translation which are not guaranteed in the original model [1, 20]. More importantly, it is observed from numerical simulations that the excitation of zonal flows is particularly strong in the MHM model in comparison with the original CHM case [11, 4, 24] where usually no dominant zonal structure is excited.

In this paper, we investigate the generation and persistence of strong and coherent large-scale anisotropic zonal structures found in the MHM model through a rigorous mathematical approach. The maintaining of a dominant single scale structure is related with the selective decay principle under proper damping forms that dissipate energy among all the other scales in a much faster rate than the particular single selected scale. The mathematical selective

decay principle for the CHM model has been developed by Majda and Wang in [13, 12]. It proves that for the quasi-geostrophic equation including rotation and stratification, only a single largest scale mode is left on the ground energy level at long time limit with damping effect and no forcing.

However, the MHM model with the important response modification in potential vorticity alters the flow dynamics in a fundamental way. The final selective states are no longer in the largest scale and always display strong anisotropic zonal structures. Here we focus on the new phenomena found from the modification made in the MHM model, that is, the decay to a purely zonal structure in the final selective decay state, and the coexistence of many intermediate transient metastable states in the decay process. The physicist's selective decay principle generally states that the solutions of the two-dimensional turbulence flow will approach to the state which minimizes the enstrophy for a given energy. From a more precise characterization about the decay process, the solution will usually visit several metastable critical points of the enstrophy with small-scale fluctuations before the final convergence to the large-scale zonal jets. We investigate the mechanism in the MHM model for the generation of coherent zonal flows by showing the following major results:

- The critical points of the enstrophy with given constant energy from the variational principle isolate the zonal mode from the other non-zonal fluctuation modes in the MHM model. Two types of exact solutions for the MHM equation can be found at the selective decay or metastable state. One is purely zonal and the other requires a special relation between the wavenumbers in the zonal and fluctuation eigenstate.
- A general form of dissipation operators is found that has the selective decay principle for the MHM model. It guarantees the convergence to one selective decay state with some particular single mode structure from any initial configuration of the state variables. On the other hand, strong ion Landau damping breaks down the selective decay to large scale state by transferring energy to small scales.
- The stable selective decay state is the purely zonal solution with zero fluctuation model. Then small perturbations in a zonal mode with low wavenumber can drive the metastable critical point solutions with non-zero fluctuations on a higher energy level to a lower energy state with only zonal structure. Usually the solution will visit several intermediate transient metastable states during the decay process.
- The number of zonal jets in the final converged zonal state is also related with the initial configuration of the state variables. The lowest wavenumber that contains non-zero energy in the initial state usually determines the final number of zonal jets.

The above results are further illustrated by a series of numerical experiments. The selective decay performance is first confirmed from solutions starting from different initial configurations. Then the additional contribution from the ion Landau damping is shown to transfer energy downscale and destroy the zonal mean structure. Besides, an additional interesting phenomena are described by an anti-damping effect to create strong large-scale condensation in one zonal mode. Together these numerical simulations characterize the many facets of the selective decay and metastability features in the MHM model.

In the structure of this paper, we first describe the general model formulations and the basic model properties in Section 2. The selective decay results for the original CHM model is briefly reviewed in Section 3. The metastability and selective decay theory for the MHM model is developed in Section 4 and 5. The permitted selective decay and metastable states are first derived from the variational principle in Section 4; while Section 5 offers the major results for the selective convergence to a single zonal stable in the MHM model. The theoretical results are illustrated with numerical simulations with various initial states and damping forms in Section 6. The conclusions are summarized in Section 7, with several more detailed calculations shown in the appendixes.

## 2 The Original and Modified Hasegawa-Mima Models

The Hasegawa-Mima (HM) model is first introduced in [6] using the adiabatic electron response on equilibrium magnetic surfaces with the Boltzmann distribution  $\exp(E/T_e)$  of electron energy  $E$ . Later, a model modification is proposed [3, 1, 18] to prevent the unphysical net radial electron transport happened in the original equation. The original *Charney-Hasegawa-Mima* (CHM) equation and the *Modified Hasegawa-Mima* (MHM) equation can be formulated under the same framework by defining a switch parameter with  $s = 0$  for CHM and  $s = 1$  for MHM as

$$\frac{\partial q}{\partial t} + J(\varphi, q) - \kappa \frac{\partial \varphi}{\partial y} = \mathcal{D}(\Delta) \varphi, \quad q = \nabla^2 \varphi - (\tilde{\varphi} + \delta_{s0} \bar{\varphi}). \quad (2.1)$$

The flows are usually projected on a two-dimensional doubly periodic geometry with  $\mathbf{x} = (x, y) \in [-L_x/2, L_x/2] \times [-L_y/2, L_y/2]$ . We use the coordinate  $x$  to represent the radial direction of the background density gradient, and  $y$  is the symmetric poloidal direction. In fusion plasma,  $\varphi(x, y, t)$  is the non-dimensionalized electrostatic potential,  $\zeta = \nabla^2 \varphi$  is the ion relative vorticity, and  $\mathbf{v}_E = -\nabla \varphi \times \hat{z} / B_0$  is the  $\mathbf{E} \times \mathbf{B}$  velocity.  $J(\varphi, q) = \partial_x \varphi \partial_y q - \partial_y \varphi \partial_x q$  is the Jacobian operator due to the flow advection  $\mathbf{v}_E \cdot \nabla q$ . And  $\kappa$  defines the constant factor describing the exponentially decaying structure in the background density along the radial direction  $n_0 \sim \exp(-\kappa x)$ . At last, the Kronecker delta  $\delta_{s_0}$  is used to remove the zonal mean state in the density response and  $\mathcal{D}(\Delta)$  introduces the generalized ion collisional viscosity and hyperviscosity, which will be discussed in details next.

In geophysical literatures [17, 22], the same CHM equation is also known as the 1.5-layer quasi-geostrophic model with  $F$ -plane effect (and conventionally with a switch of the  $x$  and  $y$  coordinates in the formulation). Then  $\kappa = -\beta$  becomes the beta-plane approximation of the Coriolis effect. The potential vorticity is usually defined as  $q = \nabla^2 \psi - F\psi$  with  $\psi$  the stream function and  $F$  describing the relative strength of rotation to stratification. The difference in the potential vorticity  $q$  here with the form in (2.1) is only subject to a scaling factor. Thus the CHM model is essentially equivalent to the 1.5-layer quasi-geostrophic model, whose properties have been studied in full detail in many previous literatures [22, 17, 8]. The rigorous theories (such as nonlinear instability and selective decay) then apply to the CHM model in exactly the same way. In the rest part of the paper, we focus on the changes introduced to the MHM model and the profound differences induced from these model adaptations.

### The model modification for stronger zonal flow and Galilean invariance

The modified Hasegawa-Mima model is developed to induce stronger zonal structures [1, 4] with an additional correction on the balanced electron response on magnetic surfaces. To achieve this, we define the zonal mean state  $\bar{f}$  by averaging along the  $y$ -direction and the fluctuation component  $\tilde{f}$  by removing the zonally-averaged mean from the original state variable (denoted as  $f$ ), that is,

$$\bar{f}(x) = \frac{1}{L_y} \int f(x, y) dy, \quad \tilde{f} = f - \bar{f}.$$

The MHM equation is modified by only removing the zonal mean electrostatic potential  $\bar{\varphi}$  in the electron response. Then the new potential vorticity in the MHM model is defined as  $q = \nabla^2 \varphi - \tilde{\varphi}$  with no zonal mean state in the second component.

Though it seems simple in the formulations of the MHM model in comparison with the CHM model, many improvements with desirable physical features can be found with this model modification [11, 1]. First, the MHM model enhances the excitation of zonal flows with more prominent zonal structures. Second, the MHM model is Galilean invariant under boosts in the  $y$  (poloidal) direction as desired for the symmetry in the poloidal direction. Further, with a constant and uniform background mean flow in the  $y$  direction,  $\bar{v}\hat{y}$ , the MHM model leads to a simple Doppler shift in the drift-wave dispersion relation  $\omega = \frac{k_y \kappa}{1+k^2} + k_y \bar{v}$ . In comparison, the original CHM model without the modification about the mean state dose not maintain these crucial properties.

### Introducing inhomogeneous damping and forcing effects

On the right hand side of the equation (2.1), we include the general damping operator  $\mathcal{D}(\Delta)$  to investigate the performance of solutions according to the dissipation mechanisms. The general dissipation operator can be formulated as a combination of different orders of the Laplace operator

$$\mathcal{D}(\Delta) \varphi = \sum_{j=0}^L d_j (-\Delta)^j (\tilde{\varphi} + \delta_{s_0} \bar{\varphi}),$$

applying on the potential function up to order  $L$ . Again,  $\delta_{s_0}$  is used to control the damping on the zonal state and the fluctuation component separately. Specifically, the zero-order term,  $d_0 \varphi$ , is related with the ion Landau damping [23],  $-d_1 \Delta \varphi$  often arises from the boundary layer effects (such as the Ekman drag),  $d_2 \Delta^2 \varphi$  represents the ion collisional friction (or Newtonian viscosity), and the higher order terms usually represent the hyperviscosity [8]. In addition, the operators act as damping effects as  $d_j > 0$ , while we can also add an anti-damping (forcing) effect into the system by using some  $d_j < 0$ .

As a typical dissipation case, we are interested in a combined form of damping and anti-damping effects

$$\begin{aligned} \mathcal{D}(\Delta)\varphi &= D(\Delta^2\varphi - 2\Delta\tilde{\varphi} + \tilde{\varphi}) + \mu(\Delta\varphi - \tilde{\varphi}) + C\varphi, \\ &= (\mu q - D\tilde{q}) + D\Delta q + C\varphi. \end{aligned} \quad (2.2)$$

Above,  $C > 0$  acting directly on the electrostatic potential  $\varphi$  is the ion Landau damping;  $D > 0$  is identified as the kinetic ion viscosity;  $\mu$ , applying directly on the potential vorticity, can act either as a forcing effect with  $\mu < 0$  or as an anti-damping (forcing) with  $\mu > 0$ . Usually,  $C$  has stronger effect on the large-scale modes, while  $D$  and  $\mu$  mostly act on the small scales. These terms can be assigned with more physical interpretations by comparing with the two-state balanced Hasegawa-Wakatani model [23, 11, 20]. There, inhomogeneous dissipation rates are applied on the relative ion density  $\Delta n$  and on the relative ion vorticity  $\Delta\zeta$ . The above damping form is recovered at the strong resistivity limit as  $\alpha \rightarrow \infty$  (so that  $\tilde{n} \rightarrow \tilde{\varphi}$ , the balanced Hasegawa-Wakatani model converges to the modified Hasegawa-Mima model [11, 20]).

## 2.1 Separated equations for the zonal mean state and fluctuations in the MHM model

In the MHM model, it can be observed that the zonal state  $\bar{\varphi}$  gets a special role separated from the fluctuation component  $\tilde{\varphi}$ . Then it is useful to rewrite the equation (2.1) in the terms of the zonal mean state and fluctuations separately. By taking the zonal average on the equation (2.1) with the special form of the damping (2.2), we find the *dynamical equation for the zonal mean state*

$$\partial_t \bar{\zeta} + \partial_x (\bar{u} \bar{\zeta}) = D \partial_x^4 \bar{\varphi} + \mu \partial_x^2 \bar{\varphi} + C \bar{\varphi}, \quad (2.3)$$

with  $\bar{\zeta} = \partial_x^2 \bar{\varphi}$  and  $\bar{u} = -\partial_y \tilde{\varphi}$ . The fluctuation feedback to the zonal mean state is through the nonlinear coupling term due to the flux

$$\partial_x (\bar{u} \bar{\zeta}) = \frac{1}{L_y} \int (\tilde{\varphi}_x \tilde{\zeta}_y - \tilde{\varphi}_y \tilde{\zeta}_x) dy.$$

In a similar way, by subtracting the mean equation (2.3) from the original model (2.1), we find the *dynamical equation for the fluctuation component*

$$\frac{\partial \tilde{q}}{\partial t} + \tilde{J}(\tilde{\varphi}, \tilde{\zeta}) - [(\partial_x + \partial_x^3) \bar{\varphi} + \kappa] \frac{\partial \tilde{\varphi}}{\partial y} + \partial_x \bar{\varphi} \frac{\partial \tilde{\zeta}}{\partial y} = C \tilde{\varphi} + \mu(\Delta - 1) \tilde{\varphi} + D(\Delta - 1)^2 \tilde{\varphi}, \quad (2.4)$$

with  $\tilde{q} = \tilde{\zeta} - \tilde{\varphi} = \nabla^2 \tilde{\varphi} - \tilde{\varphi}$ . The nonlinear fluctuation term includes the interactions between the fluctuation modes removing the zonal mean contribution

$$\tilde{J}(\tilde{\varphi}, \tilde{\zeta}) = \nabla^\perp \tilde{\varphi} \cdot \nabla \tilde{\zeta} - \partial_x (\bar{u} \bar{\zeta}).$$

Besides, the zonal mean state,  $\bar{\varphi}$ , also contributes to the fluctuations through the an additional gradient along the  $y$ -direction.

## 2.2 Conserved quantities and their dynamical equations in the MHM model

In the CHM model, two important conservative quantities [13, 16] are found as the energy  $E = \frac{1}{2} \int |\nabla\varphi|^2 + \varphi^2$  and enstrophy  $W = \frac{1}{2} \int q^2$ . Still, through the construction of the MHM model, the nonlinear term conserves both the energy and enstrophy in the same way as in the CHW equation. We can define the energy  $E$  and potential enstrophy  $W$  for the MHM model in a similar fashion as

$$E = \frac{1}{2} \int |\nabla\varphi|^2 + \varphi^2 = \frac{1}{2} \int |\nabla\tilde{\varphi}|^2 + \tilde{\varphi}^2 + |\partial_x \bar{\varphi}|^2, \quad (2.5)$$

$$W = \frac{1}{2} \int (\nabla^2\varphi - \varphi)^2 = \frac{1}{2} \int (\nabla^2\tilde{\varphi} - \tilde{\varphi})^2 + |\partial_x^2 \bar{\varphi}|^2. \quad (2.6)$$

In comparison with the original energy and enstrophy forms defined from the CHM model, (2.5) and (2.6) above get the identified fluctuation part for the potential function  $\tilde{\varphi}$ . This small modification will lead to the important difference between the zonal mean and fluctuation state solution.

The total energy and enstrophy defined in (2.5) and (2.6) for the MHM model are purely determined by the damping terms on the right hand side of (2.1). We consider the general damping form including all orders

$$\mathcal{D}(\Delta)\varphi = \sum_j d_j (-\Delta)^j (\tilde{\varphi} + \delta_{s0}\bar{\varphi}),$$

with  $s = 0$  for the damping on the entire potential function  $\varphi$ , and with  $s = 1$  only for the fluctuation modes being damped. Both the two damping forms will be found useful in the later discussions. Then we can derive the *dynamical equation for the total energy  $E$*  as

$$\begin{aligned} \frac{dE}{dt} &= - \sum_j d_j \int \varphi (-\Delta)^j (\tilde{\varphi} + \delta_{s0}\bar{\varphi}), \\ &= - \sum_j d_j \left\| (-\Delta)^{\frac{j}{2}} (\tilde{\varphi} + \delta_{s0}\bar{\varphi}) \right\|_0^2. \end{aligned} \quad (2.7)$$

with the notation  $\left\| (-\Delta)^{1/2} \varphi \right\|_0 \equiv \|\nabla\varphi\|_0$ . In a similar way, the *dynamical equation for the total enstrophy  $W$*  can be written as

$$\begin{aligned} \frac{dW}{dt} &= \sum_j d_j \int (\nabla^2\varphi - \tilde{\varphi}) (-\Delta)^j (\tilde{\varphi} + \delta_{s0}\bar{\varphi}) \\ &= - \sum_j d_j \left( \left\| (-\Delta)^{\frac{j}{2}} \nabla (\tilde{\varphi} + \delta_{s0}\bar{\varphi}) \right\|_0^2 + \left\| (-\Delta)^{\frac{j}{2}} \tilde{\varphi} \right\|_0^2 \right). \end{aligned} \quad (2.8)$$

Formally, we can rewrite  $\left\| (-\Delta)^{\frac{j}{2}} \nabla \varphi \right\|_0^2 = \left\| (-\Delta)^{\frac{j+1}{2}} \varphi \right\|_0^2$ . Notice that the second term in the enstrophy equation (2.8) only contains the fluctuation component due to the model modification. The total energy and enstrophy both keep decreasing in time from the general damping effects  $d_j > 0$ . At the same time, it can be observed from the damping terms that there is always one more differential operator  $\nabla$  for the enstrophy equation than that in the energy. This implies a faster sweep down of the enstrophy while the energy is kept in a relatively conserved quantity at suitable intermediate time scale. This sets up the foundation for the selective decay principle to be discussed in the next sections.

For a more detailed look at the energy dynamics in  $E$ , we can decompose it into the energy in the zonal mean state and the energy in fluctuations

$$E = \bar{E} + \tilde{E}, \quad \bar{E} = \frac{1}{2} \int |\partial_x \bar{\varphi}|^2 dx, \quad \tilde{E} = \frac{1}{2} \int |\nabla \tilde{\varphi}|^2 + \tilde{\varphi}^2.$$

Applying the same strategy on the mean and fluctuation equations (2.3) and (2.4) separately, we find the dynamical equations for  $\bar{E}$  and  $\tilde{E}$  correspondingly as

$$\begin{aligned} \frac{d\bar{E}}{dt} + \int \bar{v} (\overline{\tilde{u}\tilde{\zeta}}) &= - \sum_j d_j \left\| (-\Delta)^{\frac{j}{2}} \bar{\varphi} \right\|_0^2 \delta_{s0}, \\ \frac{d\tilde{E}}{dt} - \int \bar{v} (\overline{\tilde{u}\tilde{\zeta}}) &= - \sum_j d_j \left\| (-\Delta)^{\frac{j}{2}} \tilde{\varphi} \right\|_0^2. \end{aligned}$$

With  $\bar{v} = \partial_x \bar{\varphi}$  the zonally averaged velocity along  $y$ -direction. The flux term,  $\bar{v} (\overline{\tilde{u}\tilde{\zeta}})$ , on the left hand sides describes the transfer of energy between the zonal state and the fluctuation modes. The above equations are derived through simple manipulation of the mean and fluctuation dynamics with integration by parts. For further simplification, we may also represent the flux term as

$$\begin{aligned} \int \bar{v} (\overline{\tilde{u}\tilde{\zeta}}) &= - \int \bar{v} \partial_y \tilde{\varphi} (\partial_x^2 \tilde{\varphi} + \partial_y^2 \tilde{\varphi}) = - \int \bar{v} \partial_y \tilde{\varphi} \partial_x^2 \tilde{\varphi} = \int \overline{\tilde{v} \tilde{u} \tilde{v}_x} \\ &= \int \partial_x (\bar{v} \partial_y \tilde{\varphi}) \partial_x \tilde{\varphi} = - \int \partial_x \bar{v} (\overline{\tilde{u}\tilde{v}}) = \int \bar{v} \partial_x (\overline{\tilde{u}\tilde{v}}). \end{aligned}$$

The above identities characterize the energy exchange in the nonlinear flux between the energy in zonal mean and fluctuations. They are related with the zonal mean flow velocity  $\bar{v}$  and the zonal transport  $\overline{\tilde{u}\tilde{v}}$  through fluctuations.

### 3 Review of the Selective Decay for the Charney-Hasegawa-Mima Model

We first review the selective decay phenomena for the barotropic geophysical model with dissipation. The Charney-Hasegawa-Mima equation shown in (2.1) with  $s = 0$ ,

$$\frac{\partial q}{\partial t} + J(\varphi, q) - \kappa \frac{\partial \varphi}{\partial y} = \sum_j d_j (-\Delta)^j \varphi, \quad q = \nabla^2 \varphi - \varphi, \quad (3.1)$$

is equivalent to the 1.5-layer quasi-geostrophic model in geophysical turbulence. The selective decay principle predicts the convergence of any solutions of (3.1) to a single eigenstate usually with the lowest permitted energy [13]. The mathematically rigorous proof for the selective decay principle is first studied by [5, 14, 9, 15] for the Navier-Stokes equations. Then in [13, 12], the selective decay results for geophysical flows with beta-plane and  $F$ -plane effects are developed. These results for the CHM model also offer useful comparisons to distinguish the representative features that can only be discovered in the MHM model with particle response modification. Thus below we briefly summarize the major conclusions for the CHM model (3.1).

#### 3.1 Selective decay statements for the CHM model

The selective decay states refer to the critical point solutions of the enstrophy at constant energy. Then the selective decay state can be first achieved from the variational principle as the steady state solutions of the CHM model. Next, in the mathematical formulation of the selective decay principle, it is shown that the critical point solutions are indeed the long time limit of the flow state solution from the CHM model with arbitrary initial conditions. Furthermore, it predicts the stable selective decay state on the lowest permitted energy shell with base wavenumber  $k = \Lambda_1$ . In the CHM model case, there is no preference in the zonal modes and the final stable selective decay state usually contains symmetric structures in  $x$  and  $y$  directions.

In summary for the CHM model, the following conclusions can be derived rigorously based on the critical point states from the variational principle and the convergence of the ratio  $\Lambda(t) = W/E$ . For simplicity, we use the square domain with  $L_x = L_y = L$  here.

- The selective decay solution from the critical point of the enstrophy with constant energy has the structure

$$\varphi_k(t) = \sum_{k^2 = \Lambda_k} c_k e^{i(\mathbf{k} \cdot \mathbf{x} - \omega_k t)} e^{-\frac{\mathcal{D}(-\Lambda_k)}{\Lambda_k + 1} t},$$

on a single energy shell  $k^2 = \Lambda_k$ . The above state  $\varphi_k$  forms an exact solution of the CHM equation (3.1 with initial value  $c_k$ , and provides the enstrophy–energy relation,  $W(\varphi_k) = (\Lambda_k + 1)E(\varphi_k)$ . The parameter  $\kappa$  generates dispersive drift waves (or Rossby waves) with the dispersion relation  $\omega = \frac{\kappa k_y}{(2\pi/L)^2 k^2 + 1}$ . The general dissipation operator  $\mathcal{D}(\Delta)$  gives the damping effect  $\frac{\mathcal{D}(-\Lambda_k)}{\Lambda_k + 1}$  on the single energy shell.

- With the existence of non-zero viscosity,  $\sum_{j=1}^L d_j > 0$ , the generalized Dirichlet quotient  $\Lambda(t) = W(t)/E(t)$  monotonically decreases to some single energy shell of wavenumber  $k$

$$\lim_{t \rightarrow \infty} \Lambda(t) = \Lambda_k + 1 = \left(\frac{2\pi}{L}\right)^2 k^2 + 1,$$

for one single eigenvalue  $\Lambda_k$  of the Laplace operator. This further implies the convergence of any normalized solution  $\phi$  to one of the selective decay state  $\phi_k$  restricted on a single energy shell in the  $H^1$  sense

$$\lim_{t \rightarrow \infty} \|\nabla \phi - \nabla \phi_k\|_0 = 0, \quad \phi = \frac{\varphi}{\|\nabla \varphi\|_0},$$

with  $\varphi(t)$  the potential function solution from the CHM equation (3.1) with any initial condition.

- The above selective decay states associated with eigenvalues  $\Lambda_k$  on higher energy shells of wavenumbers  $k > 2$  are all unstable. Then arbitrary small perturbations from a lower energy state will drive the original Dirichlet quotient to a strictly lower energy level  $\Lambda_l + 1$  with  $l < k$ . Accordingly, the potential state  $\varphi$  will finally reach the ground state on the lowest energy shell depending on the initial symmetry.

From the above conclusions, we can see that the structure of the final selective decay state is a coherent vortex with drift waves with frequency  $\omega_k$  on the lowest permitted energy shell. Especially in the CHM model, there is no preference in the zonal modes  $k_y = 0$  and the other fluctuation modes. Thus the selective decay state is usually symmetric in  $x$  and  $y$  directions. In the next section, we will follow the same argument to derive the corresponding selective decay results for the MHM equation, where anisotropic zonal structures will always emerge in the final selective decay solutions. Before proceeding to the main results, we first illustrate the selective decay features in the CHM model using simple numerical simulations.

### 3.2 Numerical illustration of the selective decay in the CHM model

Here we use direct numerical simulations to illustrate the representative selective decay properties in the CHM model. The numerical setup is taken the same as the later test cases for the MHM model simulations shown in Section 6. The model parameters used are listed in Table 1, and we test the selective decay from the three initial states with distinct structures shown in Figure 6.1. The dissipation operator is taken as a combination of eddy viscosity (on  $\Delta^2\varphi$ ) and linear Ekman damping (on  $\Delta\varphi$ ),

$$\mathcal{D}(\Delta)q = D\Delta q = D\Delta(\Delta\varphi - \varphi),$$

where the rigorous selective decay result is guaranteed.

In the first row of Figure 3.1, the snapshots of the electrostatic potential functions  $\varphi$  at the final computational time  $t = 5000$  with the three different initial conditions are plotted. Only large scale structures remain in all the three cases, and the solutions are shifting along the  $y$ -direction in time due to the drift waves. It is found that the final structure of the selective decay state is related with the symmetry in the initial values. The first initial case has the leading Fourier mode  $(1, 0)$  and a competing mode  $(1, 1)$ . In the second initial state case where more small-scale vortices are given, the final selective decay state becomes the two leading Fourier modes  $(2, 0)$  and  $(0, 2)$ . In contrast, the third initial state with interacting double vortices with opposite signs decays to the single selective decay mode with wavenumber  $(1, 1)$ . As further comparisons, the second row of Figure 3.1 shows the corresponding time-series of the Dirichlet quotients  $\Lambda(t)$  with different initial states. In this CHM case, the Dirichlet quotients  $\Lambda(t)$  always converge to the value  $\Lambda_* = \Lambda_k + 1$  larger than 1. The slight difference in the three different initial cases corresponds to the different initial configurations for energy shells  $k^2 = 1$ ,  $k^2 = 2$ , and  $k^2 = 4$ . As a major difference in comparison with the MHM model, the CHM model has no preference in the zonal flows and always show symmetric structures in both  $x$  and  $y$  directions.

## 4 Selective Decay and Metastable Solutions from the Variational Principle

From this section, we investigate the emergence of the large-scale coherent zonal structures from the MHM model. One important feature from the model response modification is the generation of strong anisotropic zonal structures that usually cannot be observed from the CHM model. The change in the solutions of the MHM model comes from the rearrangement in the balanced potential vorticity  $q = \nabla^2\varphi - \bar{\varphi}$  by removing the zonal mean state. In the first place, we solve the *selective decay and metastable states* directly from the variational principle, which is the state with the critical value of enstrophy at fixed energy level.

From the *physical selective decay principle*, a selective decay state  $\varphi^*$  refers to a critical point of the enstrophy at constant energy level. From the previous definitions of the conserved energy and enstrophy (2.5) and (2.6) in the MHM model, the critical point state satisfies the variational principle

$$E(\varphi^*) = E, \quad \frac{\delta W}{\delta\varphi} \Big|_{\varphi^*} = \Lambda \frac{\delta E}{\delta\varphi} \Big|_{\varphi^*}, \quad (4.1)$$

with  $\Lambda$  as the Lagrangian multiplier. More precisely, we only refer the stable critical solution as the final selective decay state, while the unstable saddle points as the metastable solutions of the system. Next, we find the variational derivatives for the energy and enstrophy defined for the MHM model; then derive the explicit form of the invariant selective decay solution based on the critical point and dissipation forms.

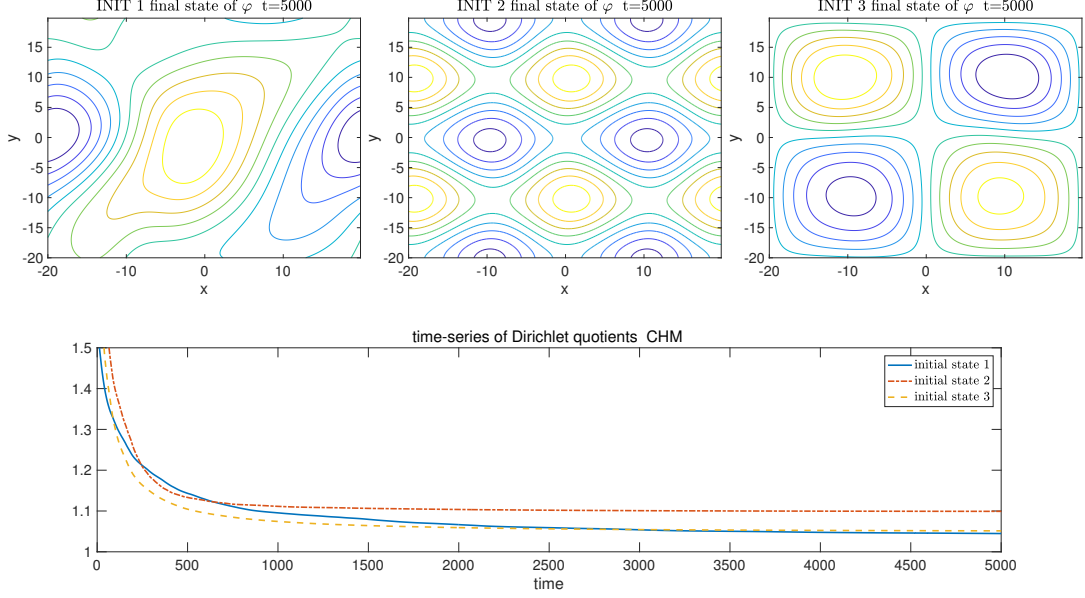


Figure 3.1: Snapshots of the electrostatic potential functions  $\varphi$  at final time from the CHM model simulations, together with the time-series of the Dirichlet quotients with three different initial states.

#### 4.1 Variational derivatives for the modified energy and enstrophy

We start directly from the definitions of the energy and enstrophy in (2.5) and (2.6). The variational derivatives of a functional  $\mathcal{F}(u)$  can be calculated from the directional derivatives under the inner product  $(u, v)_0 = \int uv$  in Hilbert space so that

$$\left( \frac{\delta \mathcal{F}}{\delta u}, \delta u \right)_0 \equiv \lim_{\epsilon \rightarrow \infty} \frac{\mathcal{F}(u + \epsilon \delta u) - \mathcal{F}(u)}{\epsilon}.$$

First for the energy variations, considering the small variations in the potential  $\varphi + \epsilon \delta \varphi$ , and vorticity  $\zeta + \epsilon \delta \zeta$ , with  $\delta \zeta = \Delta \delta \varphi$ , we calculate directly from the definition

$$\frac{1}{\epsilon} [E(\varphi + \epsilon \delta \varphi) - E(\varphi)] = (-\zeta + \tilde{\varphi}, \delta \varphi)_0 + O(\epsilon).$$

The above relation is direct result from an integration by parts  $\int \varphi \delta \zeta = \int \zeta \delta \varphi$  and noticing  $\int \tilde{\varphi} \delta \tilde{\varphi} = \int \tilde{\varphi} \delta \varphi$ . Taking the limit  $\epsilon \rightarrow 0$ , the left hand side of the equation above defines the variational derivative through the inner product  $\left( \frac{\delta E}{\delta \varphi}, \delta \varphi \right)_0$ . In a similar way, we can find the variational derivative for the enstrophy through a direct calculation

$$\frac{1}{\epsilon} [W(\varphi + \epsilon \delta \varphi) - W(\varphi)] = (\Delta \zeta - 2\tilde{\zeta} + \tilde{\varphi}, \delta \varphi)_0 + O(\epsilon).$$

Therefore, we find the variational derivatives for the energy and enstrophy as

$$\begin{aligned} \frac{\delta E}{\delta \varphi} &= -\zeta + \tilde{\varphi}, \\ \frac{\delta W}{\delta \varphi} &= \Delta \zeta - 2\tilde{\zeta} + \tilde{\varphi}. \end{aligned} \tag{4.2}$$

Notice that if we remove the tildes in the above identities in (4.2), they go back the variational derivatives for the CHM model energy and enstrophy accordingly [13].

Next, put the variational derivatives back to the Euler-Lagrangian equation (4.1) with the Lagrangian multiplier  $\Lambda$ . The critical solution  $(\zeta^*, \varphi^*)$  satisfies the equation

$$\begin{aligned} \Delta \zeta^* - 2\tilde{\zeta}^* + \tilde{\varphi}^* &= -\Lambda \zeta^* + \Lambda \tilde{\varphi}^* \\ \Rightarrow (\Delta - 1 + \Lambda)(1 - \Delta) \tilde{\varphi}^* &= (\partial_x^2 + \Lambda) \partial_x^2 \tilde{\varphi}^*. \end{aligned}$$

We rearrange the above equation by putting the fluctuation modes on the left side and the zonal mean state on the right. To solve the above equation, again by taking the zonal average on both sides, we find the equation for the zonal mean state; then the solution for the fluctuation modes follows by subtracting the zonal mean equation. Therefore the critical point state should satisfy the following form in mean and fluctuation components

$$\begin{aligned}\partial_x^2 \bar{\varphi}^* &= -\Lambda \bar{\varphi}^*, \\ \Delta \tilde{\varphi}^* &= -(\Lambda - 1) \tilde{\varphi}^*.\end{aligned}\tag{4.3}$$

In the MHM model case, the eigenvalues for the zonal state  $\bar{\varphi}$  and the fluctuations  $\tilde{\varphi}$  have a difference of 1. Directly from the above equations (4.3), the critical energy and enstrophy satisfy the relation

$$W^* = \frac{1}{2} \int (\zeta^* - \tilde{\varphi}^*)^2 = \frac{1}{2} \Lambda^2 \int (\tilde{\varphi}^* + \bar{\varphi}^*)^2 = \Lambda E^*.\tag{4.4}$$

Note that the CHM and MHM models get the same critical energy–enstrophy relation, but with different critical states [13]. The Lagrangian multiplier  $\Lambda$  could be different in the two models. Similarly, we arrive at the results that the ground state with minimum  $\Lambda^* = \Lambda_1 + 1$  (where  $\Lambda_1$  is the minimum value of the Laplace operator) gives the minimizer of the enstrophy  $W$  given the energy  $E$  with non-zero fluctuations. Still the zonal solutions in (4.3) give a series of permitted selective decay states.

## 4.2 Exact solutions from the metastable and selective decay states

We can find the eigenfunctions from the equations in (4.3) and verify that they form the exact solutions for the mean and fluctuation equations of the MHM model. First we solve *the solution of the zonal mean state*

$$\bar{\varphi} = A(t) \cos \sqrt{\Lambda} x + B(t) \sin \sqrt{\Lambda} x, \quad \bar{\zeta} = \partial_x^2 \bar{\varphi} = -\Lambda \bar{\varphi}.\tag{4.5}$$

The coefficients  $(A, B)$  can be then determined by the zonal mean equation (2.3) with the dissipation form in (2.2)

$$\partial_t \bar{\varphi} = -(D\Lambda + C\Lambda^{-1} - \mu) \bar{\varphi}.$$

The fluctuation feedback  $\partial_x (\overline{\tilde{u}\tilde{\zeta}})$  from the non-zonal modes is found to be zero from the eigenfunction of the fluctuation modes (in fact,  $\overline{\tilde{u}\tilde{\zeta}} = \Lambda_k \int \tilde{\varphi} \partial_y \tilde{\varphi} dy = 0$ ). Therefore the solution of zonal state (4.5) is persistent with the following exponential decay profile

$$A(t) = A_0 e^{-(D\Lambda + C\Lambda^{-1} - \mu)t}, \quad B(t) = B_0 e^{-(D\Lambda + C\Lambda^{-1} - \mu)t},$$

with  $(A_0, B_0)$  the initial values of the zonal mean state. Indeed, we can see from the exact solution that the parameter  $\mu > 0$  increases the energy in the zonal state while the parameters  $D$  and  $C$  dissipate the energy. In addition,  $D$  has stronger effect on the smaller scales in high wavenumber modes and  $C$  acts strongest on the large scale modes.

Then by solving the second equation for the fluctuations, we found *the solution of the fluctuation component*

$$\tilde{\varphi} = \sum_{k^2 = \text{const.}} c_{\mathbf{k}}(t) e^{i \frac{2\pi}{L} \mathbf{k} \cdot \mathbf{x}}, \quad \tilde{\zeta} = \Delta \tilde{\varphi} = -\Lambda_k \tilde{\varphi},\tag{4.6}$$

with  $\mathbf{k} = (k_x, k_y) \in \mathbb{Z}^2$  and  $|\mathbf{k}| = k$  on a constant energy shell. Especially, we find that the permitted eigenvalues for the critical solutions satisfy

$$\Lambda - 1 = \Lambda_k \equiv \left( \frac{2\pi}{L_x} k_x \right)^2 + \left( \frac{2\pi}{L_y} k_y \right)^2, \quad \Lambda > 1,\tag{4.7}$$

where  $(k_x, k_y)$  are integers and  $(L_x, L_y)$  are important model parameters defines the domain size in  $x$  and  $y$  directions. We also get the constraint in the eigenvalue  $\Lambda \geq 1 + (2\pi/L)^2$  for all the nontrivial fluctuation state. It is easy to check the zonal mean solution (4.5) also has no contribution in the nonlinear interaction terms  $\tilde{J}(\varphi, q) = 0$

in the fluctuation equation (2.4) under the eigenvalue constraint (4.7). The equation for the coefficient  $c_k$  can be found from the fluctuation equation for  $\tilde{q} = \zeta - \tilde{\varphi} = -\Lambda\tilde{\varphi}$

$$\frac{dc_k}{dt} + i\frac{2\pi}{L_y}k_y\kappa\Lambda^{-1}c_k = -(D\Lambda + C\Lambda^{-1} - \mu)c_k.$$

The solution for the coefficient  $c_k$  can be written as

$$c_k(t) = c_k(0)e^{-i\omega_k t - d_k t}, \quad \omega_k = \frac{2\pi}{L_y}k_y\kappa\Lambda^{-1}, \quad d_k = D\Lambda + C\Lambda^{-1} - \mu.$$

Obviously, the non-zero density gradient  $\kappa$  generates drift waves in the solution. Above  $\omega_k$  is the frequency for the drift waves induced for the fluctuation modes with  $k_y \neq 0$ . The damping rate in the fluctuation and in the zonal mode stays in the same form for the same eigenstate.

*Remark.* (different domain sizes with aspect ratio  $\alpha = L_y/L_x$ ) From the above argument, it can be found that the critical state is valid for any rectangular domain size with aspect ratio  $\alpha$  though we usually consider the square domain case  $L = L_x = L_y$  in the following discussions. In fact, the only difference from the elongated  $x$  or  $y$  direction is the introduction of more intermediate modes between the original integer wavenumber values. These additional modes will induce more complicated nonlinear interactions between different scales during the transient states in the decay process, while the same final selective decay state will be reached as the energy inside all the other modes are dissipated. The effect with different aspect ratios is discussed with numerical results in [20].

### *The practical selective decay state with periodic boundary condition*

More attention is needed in treating the zonal selective decay solution (4.5) given the periodic boundary condition. To enforce the periodicity at the boundary points  $x = \pm\frac{L}{2}$ , the permitted solution then must be in the form

$$\bar{\varphi} = A \cos \sqrt{\Lambda_k + 1}x,$$

for any values of  $\sqrt{\Lambda} = \sqrt{\Lambda_k + 1}$  not an integer. But the constraint for the zonal eigenstate  $\bar{\varphi}$  in the above form is only for the case with non-zero fluctuation modes  $\tilde{\varphi}$ . As another alternative, the eigenstate only has a single zonal mode with zero fluctuation. Then any wavenumber is permitted. Both of the solutions satisfy the MHM equation (2.1) and are valid for the variational principle in (4.1) that minimizes the enstrophy with constant energy. Therefore we summarize the two different kinds of critical point solutions as follows.

**Proposition 1.** *The selective decay or metastable solution for the MHM model (2.1) has either of the following two forms:*

- *If there exists non-zero fluctuation modes  $k_y \neq 0$  with drift waves in the critical state, the only permitted solution from the variational principle with periodic boundary condition satisfies the structure*

$$\bar{\varphi} = A_0 e^{-d_k t} \cos \sqrt{\Lambda}x, \quad \tilde{\varphi} = \sum_{k^2=\text{const.}} c_{\mathbf{k},0} e^{-i\omega_k t - d_k t} e^{i\frac{2\pi}{L}\mathbf{k}\cdot\mathbf{x}}, \quad \Lambda - 1 = \Lambda_k \equiv \left(\frac{2\pi}{L}\right)^2 k^2, \quad (4.8)$$

*with  $d_k$  the total damping effects and  $\omega_k$  the drift-wave frequency.*

- *If there is a purely zonal flow state with  $k_y = 0$  in the critical state, the solution can have the general zonal form varying along the  $x$ -direction for some integer number  $l$*

$$\bar{\varphi}_l = A_0 e^{-d_k t} \cos\left(l\frac{2\pi}{L}x\right) + B_0 e^{-d_k t} \sin\left(l\frac{2\pi}{L}x\right), \quad \tilde{\varphi} \equiv 0. \quad (4.9)$$

*This critical point solution is more likely to become the final selective decay state from the numerical simulations, considering that the non-zonal fluctuations keep breaking into the zonal modes due to the nonlinear interactions.*

Therefore the general solution of the MHM model can be written as the summation of either the above eigenfunctions (4.8) or (4.9). In the second case, there is only non-zero zonal state and the zonal wavenumber does not need to be larger than 1.

## 5 Selective Decay Principle for the Modified Hasegawa-Mima Model

In this section, we consider the mathematical formulation for the selective decay of the MHM model. Previously, the solutions (4.8) and (4.9) are directly achieved from the variational principle and are checked to satisfy the MHM equation. The next question is whether arbitrary initial states will converge to these selective decay solutions. Especially, we would like to find the proper dissipation forms that can guarantee the selective delay with arbitrary initial conditions.

In constructing the proper dissipation forms that drive the system to the selective decay state, the key quantity is the *Dirichlet quotient*  $\Lambda(t)$  defined as the ratio between the enstrophy and energy

$$\Lambda(t) = \frac{W(t)}{E(t)}. \quad (5.1)$$

It quantifies the decay rates of modes among different scales during the evolution of the system (this  $\Lambda(t)$  should not be confused with the previous eigenvalue  $\Lambda$ ). Then if the Dirichlet quotient  $\Lambda(t)$  converges to some corresponding eigenvalue  $\Lambda_*$ , it implies the mathematical selective decay to some exact eigenvalue solution in (4.8) or (4.9). At last, we have the convergence to one of the selective decay state  $\varphi_k$  for the normalized potential function in the  $H^1$  sense

$$\lim_{t \rightarrow \infty} \|\nabla\phi - \nabla\phi_k\|_0 = 0, \quad \phi = \frac{\varphi}{\|\nabla\varphi\|_0}, \quad (5.2)$$

from the convergence of  $\Lambda(t)$ . The rigorous argument for (5.2) will be exactly the same as the convergence in the CHM model once we have the monotonic convergence of the Dirichlet quotient. It requires careful comparisons for the lower and higher modes projected to different energy levels calculated in details in [12]. In this section, we first check the energy-enstrophy decay based on the Dirichlet quotient. Then the selective decay principle can be derived based on the final convergence of the Dirichlet quotient  $\Lambda(t)$  to one of the eigenvalues.

To display the major conclusions in the first place, we state the following theorem for the mathematical selective decay principle:

**Theorem 2.** (*selective decay for the modified Hasegawa-Mima model*) For the MHM model (2.1) with modified vorticity  $q = \nabla^2\varphi - \tilde{\varphi}$  and with a combination of each order of damping operators  $\mathcal{D}(\Delta)$ , the selective decay principle holds for arbitrary initial data in the sense of (5.2) when the Dirichlet quotient  $\Lambda(t)$  monotonically decreases to an eigenvalue  $\Lambda_*$ . For several specific dissipation forms of  $\mathcal{D}(\Delta)$ , we have the following conclusions according to the time evolution of the Dirichlet quotient  $\Lambda(t)$ :

- In the first-order linear damping  $-D_1q$ , there is no selective decay effect. In this case, the energy  $E$  and enstrophy  $W$  both have the same exponential decay in the same rate, and Dirichlet quotient  $\Lambda(t) \equiv \Lambda(0)$  conserves in time.
- The selective decay is enhanced with the second-order damping form

$$\mathcal{D}(\Delta)\varphi = D_2(\Delta q - \tilde{q}).$$

The second part in the dissipation relating only the fluctuation is essential in guaranteeing the selective decay. In addition, the combination of the first and second order damping form

$$\mathcal{D}(\Delta)\varphi = D(\Delta q + \partial_x^2\tilde{\varphi}) = D(\Delta q - \tilde{q}) + Dq,$$

also guarantees the monotonically decreasing property of the quotient  $\Lambda(t)$ , while the energy and enstrophy may increase when the second term,  $D_2 > 0$ , gives the anti-damping effect.

- The linear Landau damping  $C_0\varphi$  increases the Dirichlet quotient  $\Lambda(t)$  by strongly dissipating the largest scales. This means that the Landau damping moves energy down spectrum to small scales and usually breaks the selective decay state. In a combination with the second-order damping form

$$\mathcal{D}(\Delta)\varphi = C_0\varphi + D_2(\Delta q - \tilde{q}),$$

the selective decay is resumed only when the Landau damping strength is small enough

$$C_0 \leq D_2\Lambda_1^2.$$

- A general dissipation operator that gives the selective decay principle can be constructed in the following form

$$\mathcal{D}(\Delta)\varphi = -\sum_{j \geq 1} D_j \left[ (-\Delta + 1)^j \tilde{\varphi} + (-\partial_x^2)^j \bar{\varphi} \right],$$

with  $D_j \geq 0$  for  $j \geq 2$  and  $D_1$  as any constant values.

## 5.1 Bounds and dynamics of the Dirichlet quotient

We can first find the lower bound for the Dirichlet quotient  $\Lambda(t)$ . From the definitions of energy and enstrophy in (2.5) and (2.6), the Dirichlet quotient can be written explicitly as

$$\Lambda(t) = \frac{\|\nabla^2 \tilde{\varphi} - \bar{\varphi}\|^2 + \|\partial_x^2 \bar{\varphi}\|^2}{\|\nabla \tilde{\varphi}\|^2 + \|\bar{\varphi}\|^2 + \|\partial_x \bar{\varphi}\|^2}.$$

A simple application of Poincaré inequality,  $\|\nabla^2 \tilde{\varphi}\|^2 + \|\nabla \tilde{\varphi}\|^2 \geq \Lambda_1 (\|\nabla \tilde{\varphi}\|^2 + \|\tilde{\varphi}\|^2)$ , and  $\|\partial_x^2 \bar{\varphi}\|^2 \geq \Lambda_1 \|\partial_x \bar{\varphi}\|^2$  gives

$$\Lambda(t) \geq \Lambda_1,$$

with  $\Lambda_1 = \left(\frac{2\pi}{L}\right)^2$  the smallest eigenvalue of the Laplace operator. So as long as we can show that the quotient  $\Lambda(t)$  is monotonically decreasing in time, and together with that  $\Lambda(t)$  has a lower bound, we know that  $\Lambda(t)$  converges to some limit as  $t \rightarrow \infty$ , that is,

$$\Lambda(t) \rightarrow \Lambda_* \geq \Lambda_1.$$

Next, it is relatively easy to show that  $\Lambda(t)$  converges to some eigenvalue  $\Lambda_k + 1$  or  $\Lambda_l$  from the dynamical equation of  $\Lambda(t)$ . In the first part of this section, we derive the dynamical equation for the Dirichlet quotient  $\Lambda(t)$ , and discuss its decaying property from the dynamics of energy and enstrophy.

### 5.1.1 Dynamical equation for the Dirichlet quotient

Consider the dissipation in one single order  $j$  acting on either the entire variable or just the fluctuation component

$$\mathcal{D}_j \varphi = d_j (-\Delta)^j \varphi, \quad \tilde{\mathcal{D}}_j \varphi = d_j (-\Delta)^j \tilde{\varphi}.$$

The corresponding energy and enstrophy equations from (2.7) and (2.8) then become

$$\frac{dE}{dt} = -d_j \left\| (-\Delta)^{\frac{j}{2}} \varphi \right\|_0^2, \quad \frac{dW}{dt} = -d_j \left( \left\| (-\Delta)^{\frac{j+1}{2}} \varphi \right\|_0^2 + \left\| (-\Delta)^{\frac{j}{2}} \tilde{\varphi} \right\|_0^2 \right),$$

for  $\mathcal{D}_j \varphi$ , and

$$\frac{dE}{dt} = -d_j \left\| (-\Delta)^{\frac{j}{2}} \tilde{\varphi} \right\|_0^2, \quad \frac{dW}{dt} = -d_j \left( \left\| (-\Delta)^{\frac{j+1}{2}} \tilde{\varphi} \right\|_0^2 + \left\| (-\Delta)^{\frac{j}{2}} \bar{\varphi} \right\|_0^2 \right),$$

for  $\tilde{\mathcal{D}}_j \varphi$ . By directly taking the derivative for the Dirichlet quotient  $\Lambda(t)$ , we find the dynamical equation from the energy and enstrophy dynamics for a single damping term with  $j \geq 1$

$$\begin{aligned} \frac{d\Lambda}{dt} &= \frac{1}{E^2} (E\dot{W} - \dot{E}W) = \frac{1}{E} (\dot{W} - \Lambda\dot{E}) \\ &= -\frac{d_j}{E} \left[ \left( \left\| (-\Delta)^{\frac{j+1}{2}} \tilde{\varphi} \right\|_0^2 - \Gamma(t) \left\| (-\Delta)^{\frac{j}{2}} \tilde{\varphi} \right\|_0^2 \right) \right. \\ &\quad \left. + \left( \left\| (-\partial_x^2)^{\frac{j+1}{2}} \bar{\varphi} \right\|_0^2 - \Lambda(t) \left\| (-\partial_x^2)^{\frac{j}{2}} \bar{\varphi} \right\|_0^2 \right) \right], \end{aligned} \tag{5.3}$$

by introducing  $\Gamma(t) = \Lambda(t) - 1$ . The above equation (5.3) is from the full damping operator  $\mathcal{D}_j \varphi$ , and the last row for damping on the zonal mean state will vanish if we only consider the damping on fluctuations  $\tilde{\mathcal{D}}_j \varphi$ . For

simplicity in notation, we also introduce the new quantities

$$U_j = \bar{U}_j + \tilde{U}_j, \quad \begin{aligned} \bar{U}_j &= \left\| (-\partial_x^2)^{\frac{j}{2}} \bar{\varphi} \right\|_0^2 - \Lambda(t) \left\| (-\partial_x^2)^{\frac{j-1}{2}} \bar{\varphi} \right\|_0^2, \\ \tilde{U}_j &= \left\| (-\Delta)^{\frac{j}{2}} \tilde{\varphi} \right\|_0^2 - \Gamma(t) \left\| (-\Delta)^{\frac{j-1}{2}} \tilde{\varphi} \right\|_0^2. \end{aligned} \quad (5.4)$$

Then, we can rewrite the dynamical equations (5.3) in the compact form

$$\begin{aligned} \frac{d\Lambda}{dt} &= -\frac{d_j}{E} \left( \tilde{U}_{j+1} + \bar{U}_{j+1} \right), \quad \text{with } \mathcal{D}_j \varphi = d_j (-\Delta)^j \varphi, \\ \frac{d\Lambda}{dt} &= -\frac{d_j}{E} \tilde{U}_{j+1}, \quad \text{with } \tilde{\mathcal{D}}_j \varphi = d_j (-\Delta)^j \tilde{\varphi}. \end{aligned}$$

Due to the linear structure, the dynamics with different orders of dissipation forms  $\mathcal{D}_j \varphi$  can be added together from the above single contribution with each individual damping. In general, it is difficult to determine the signs in the terms  $U_{j+1}$  and  $\tilde{U}_{j+1}$  on the right hand sides of the above dynamics. Next, we try to reorganize these terms through several useful identities from the Dirichlet quotient.

### 5.1.2 Useful equalities from the Dirichlet quotient

Using the definition of the Dirichlet quotient  $\Lambda(t)$ , we find the following useful equality

$$\begin{aligned} \int \left( \tilde{\zeta}^2 + \tilde{\varphi}^2 + 2|\nabla \tilde{\varphi}|^2 + \bar{\zeta}^2 \right) &= \Lambda(t) \int \left( |\nabla \tilde{\varphi}|^2 + \tilde{\varphi}^2 + |\partial_x \bar{\varphi}|^2 \right), \\ \int \left( \tilde{\zeta}^2 - \Gamma |\nabla \tilde{\varphi}|^2 \right) + \int \left( \bar{\zeta}^2 - \Lambda |\partial_x \bar{\varphi}|^2 \right) &= - \int \left( |\nabla \tilde{\varphi}|^2 - \Gamma \tilde{\varphi}^2 \right). \end{aligned}$$

The second row is through a simple rearrangement of the previous equality in the zonal and fluctuation parts and using the relation  $\Lambda(t) = \Gamma(t) + 1$ . The two terms on the left hand side can be further reorganized through an integration by parts. The fluctuation part becomes

$$\begin{aligned} \int \left( \tilde{\zeta}^2 - \Gamma |\nabla \tilde{\varphi}|^2 \right) &= \int \left| \tilde{\zeta} + \Gamma \tilde{\varphi} \right|^2 - 2\Gamma \tilde{\varphi} \Delta \tilde{\varphi} - \Gamma^2 \tilde{\varphi}^2 - \Gamma |\nabla \tilde{\varphi}|^2 \\ &= \int \left| \tilde{\zeta} + \Gamma \tilde{\varphi} \right|^2 + \Gamma \int \left( |\nabla \tilde{\varphi}|^2 - \Gamma \tilde{\varphi}^2 \right). \end{aligned}$$

In a similar way, we also have the identity for the the zonal mean state part as

$$\int \left( \bar{\zeta}^2 - \Lambda |\partial_x \bar{\varphi}|^2 \right) = \int \left| \bar{\zeta} + \Lambda \bar{\varphi} \right|^2 + \Lambda \int \left( |\partial_x \bar{\varphi}|^2 - \Lambda \bar{\varphi}^2 \right).$$

Combining all the above relations together and again using  $\Gamma(t) + 1 = \Lambda(t)$ , we find the useful identity relating the different damping effects

$$\left\| \tilde{\zeta} + \Gamma \tilde{\varphi} \right\|_0^2 + \left\| \bar{\zeta} + \Lambda \bar{\varphi} \right\|_0^2 = -\Lambda \left[ \left( \|\nabla \tilde{\varphi}\|_0^2 - \Gamma \|\tilde{\varphi}\|_0^2 \right) + \left( \|\partial_x \bar{\varphi}\|_0^2 - \Lambda \|\bar{\varphi}\|_0^2 \right) \right]. \quad (5.5)$$

For simplicity, we can rewrite the above relation (5.5) by introducing the new notations

$$S_1 = \tilde{S}_1 + \bar{S}_1 = -\Lambda U_1,$$

where  $U_1$  is defined in in (5.4) and the non-negative pairs for the fluctuation and zonal mean state are defined in general as

$$\tilde{S}_j = \left\| (-\Delta)^{\frac{j+1}{2}} \tilde{\varphi} - \Gamma (-\Delta)^{\frac{j-1}{2}} \tilde{\varphi} \right\|_0^2, \quad \bar{S}_j = \left\| (-\partial_x^2)^{\frac{j+1}{2}} \bar{\varphi} - \Lambda (-\partial_x^2)^{\frac{j-1}{2}} \bar{\varphi} \right\|_0^2. \quad (5.6)$$

Following the same trick with integration by parts, we can find the useful recursive relations for the above quantities in the more general form

$$\tilde{U}_{j+1} = \tilde{S}_j + \Gamma \tilde{U}_j, \quad \bar{U}_{j+1} = \bar{S}_j + \Lambda \bar{U}_j. \quad (5.7)$$

Notice the difference in the coefficients  $\Lambda(t) = \Gamma(t) + 1$  in the fluctuation and zonal mean state. A detailed calculation about the above identities are shown in Appendix A. These equalities will be used repeatedly next for the derivation of proper dynamical equation for the Dirichlet quotient  $\Lambda(t)$  under different damping forms.

## 5.2 The dissipation operators for the selective decay

Now we show the proper dissipation operators that can monotonically reduce the value of the Dirichlet quotient  $\Lambda(t)$  as the system evolves in time. As one of the major difference in the MHM model in comparison with the CHM model, the separate roles of the zonal and fluctuation modes need to be identified here. We will begin with the typical damping cases introduced in (2.2), and then show a general damping form including all higher order terms that can guarantee the selective decay principle.

### 5.2.1 The first and second order dissipation operators

In the first case, we consider the simplest linear damping on the potential vorticity

$$\mathcal{D}(\Delta)\varphi = -D_1 q = -D_1(\Delta\varphi - \tilde{\varphi}). \quad (5.8)$$

It can be compared with the Ekman damping in geophysical flows. From the dynamical equation (5.3) for the general form, we can immediately find the dynamical equation for the Dirichlet quotient in this first order case as

$$\frac{d\Lambda}{dt} = -\frac{D_1}{E} (U_2 + \tilde{U}_1),$$

with the notations  $U_j$  and  $\tilde{U}_j$  defined in (5.4). Then using the equality (5.7), it can be found that the total damping effect on the right hand side actually vanishes in this case

$$\begin{aligned} \tilde{U}_2 &= \tilde{S}_1 + \Gamma\tilde{U}_1, \quad \bar{U}_2 = \bar{S}_1 + \Lambda\bar{U}_1 \\ \Rightarrow U_2 + \tilde{U}_1 &= S_1 + \Lambda U_1 = 0, \end{aligned}$$

where the relation  $\Lambda = \Gamma + 1$  and the identity  $S_1 = -\Lambda U_1$  in (5.5) are applied. This shows that the Dirichlet quotient in the linear damping case (5.8) is conserved in time, so that it can be determined from the initial value

$$\frac{d\Lambda}{dt} = 0 \Rightarrow \Lambda(t) = \Lambda(0). \quad (5.9)$$

Furthermore, notice that this conclusion is valid for either positive or negative values of the coefficient  $D_1$ . This result is no surprise since in this linear damping case, both the energy and enstrophy dynamics become linear

$$\frac{dE}{dt} = -D_1 E, \quad \frac{dW}{dt} = -D_1 W.$$

This implies that the enstrophy and energy both decay at the same rate at every scale, with  $W(t) = \Lambda(0)E(t)$ . This shows that the initial values at each scale decay at the same rate. Thus there is no selective decay for a particular scale in this linear damping case.

Next, we consider the second-order viscosity with the Laplacian operator on the potential vorticity in the form

$$\mathcal{D}(\Delta)\varphi = -D_2(-\Delta q + \tilde{q}) = -D_2(-\Delta^2\varphi + 2\Delta\tilde{\varphi} - \tilde{\varphi}). \quad (5.10)$$

This is the similar form as the Newtonian eddy viscosity. In a similar way as before using the general dynamics (5.3), we find the dynamical equation for the Dirichlet quotient in this second order damping case as

$$\frac{d\Lambda}{dt} = -\frac{D_2}{E} (U_3 + 2\tilde{U}_2 + \tilde{U}_1).$$

Using again the equality in (5.7) repeatedly, the damping terms on the right hand side can be reorganized in the form as

$$\begin{aligned} U_3 &= S_2 + \Gamma\tilde{U}_2 + \Lambda\bar{U}_2, \quad \tilde{U}_2 = \tilde{S}_1 + \Gamma\tilde{U}_1, \quad \bar{U}_2 = \bar{S}_1 + \Lambda\bar{U}_1 \\ \Rightarrow U_3 + 2\tilde{U}_2 + \tilde{U}_1 &= S_2 + \tilde{S}_1 + \Lambda(S_1 + \Lambda U_1) = S_2 + \tilde{S}_1. \end{aligned}$$

Therefore in the second-order damping case (5.10), the Dirichlet quotient follows the dynamical equation with strictly non-positive terms on the right hand side as

$$\frac{d\Lambda}{dt} = -\frac{D_2}{E} \left( \left\| \nabla\tilde{\zeta} + \Gamma\nabla\tilde{\varphi} \right\|_0^2 + \left\| \partial_x\bar{\zeta} + \Lambda\partial_x\bar{\varphi} \right\|_0^2 + \left\| \tilde{\zeta} + \Gamma\tilde{\varphi} \right\|_0^2 \right). \quad (5.11)$$

The quotient  $\Lambda(t)$  is monotonically decreasing until it reaches the minimum  $\Lambda_*$ . Then the final state should converge to a corresponding eigenstate  $\nabla^2 \tilde{\varphi}_* = -\Gamma_* \tilde{\varphi}_*$  and  $\partial_x^2 \bar{\varphi}_* = -\Lambda_* \bar{\varphi}_*$ , where every term on the right hand side of (5.11) vanishes. We will discuss the more rigorous proof for this convergence next in Section 5.3. On the other hand, it can be found that the second component,  $-D_2 \tilde{q}$ , only on the fluctuation component is essential in maintaining the strictly decreasing property of the Dirichlet quotient. In Appendix B, we give a simple counter-example using only the damping operator  $D\Delta q$ , where it is shown that with particular initial state, the Dirichlet quotient will increase in time. Thus the selective decay might be violated in that case.

In addition, we may also consider the combined effects from the previous two damping cases (5.8) and (5.10), making use of the fact that the linear damping  $-D_1 q$  will not alter the value of  $\Lambda(t)$ . Therefore, the above dynamical equation (5.11) is still valid for the combined damping form

$$\mathcal{D}(\Delta)\varphi = -D_2(-\Delta q + \tilde{q}) - D_1 q = D_2 \Delta q + (D_2 + D_1)(\Delta \tilde{\varphi} + \tilde{\varphi}) - D_1 \partial_x^2 \bar{\varphi},$$

for any constant value  $D_1$ . Especially, by taking  $D_1 = -D_2$ , we find that the selective decay damping with the Laplace operator on the potential vorticity becomes  $D_2(\Delta q + \partial_x^2 \bar{\varphi})$ . Further notice that when  $D_1 < 0$ , the second part  $D_1 q$  actually acts as an anti-damping (forcing) effect to increase both energy and enstrophy.

### 5.2.2 The effect from ion Landau damping

Another interesting case is to introduce the effect of the ion Landau damping [23] as a linear constant directly applying on the potential function

$$\mathcal{D}\varphi = C_0 \varphi.$$

The Landau damping  $C_0$  usually has stronger damping effect on the large scales and weaker on the small scales. As a result, it may have the effect to increase the portion of energy among small scales. Accordingly, we can find the dynamical equation for the Dirichlet quotient with only Landau damping as

$$\frac{d\Lambda}{dt} = \frac{C_0}{\Lambda E} \left( \|\tilde{\zeta} + \Gamma \tilde{\varphi}\|_0^2 + \|\bar{\zeta} + \Lambda \bar{\varphi}\|_0^2 \right). \quad (5.12)$$

Indeed, the value of  $\Lambda(t) = W/E$  becomes monotonically increasing in time with the pure effect of the Landau damping  $C_0 > 0$ . This means that the Landau damping induces the forward energy cascade down the spectrum. Then no selective decay to a dominant large scale mode can be expected with the pure effect of Landau damping.

In real applications, the Landau damping is usually combined together with other dissipation effects [1, 11]. Here, consider the dissipation form including the second-order damping in (5.10) and the Landau damping effect

$$\mathcal{D}(\Delta)\varphi = -D_2(-\Delta q + \tilde{q}) + C_0 \varphi. \quad (5.13)$$

Combining equations (5.11) and (5.12) together, the new dynamical equation with the damping form (5.13) becomes

$$\begin{aligned} \frac{d\Lambda}{dt} &= -\frac{D_2}{E} \left( \|\nabla \tilde{\zeta} + \Gamma \nabla \tilde{\varphi}\|_0^2 + \|\partial_x \bar{\zeta} + \Lambda \partial_x \bar{\varphi}\|_0^2 \right) \\ &\quad + \frac{1}{E} (C_0 \Lambda^{-1} - D_2) \|\tilde{\zeta} + \Gamma \tilde{\varphi}\|_0^2 + \frac{C_0}{\Lambda E} \|\bar{\zeta} + \Lambda \bar{\varphi}\|_0^2 \\ &\leq \frac{1}{E} (C_0 \Lambda^{-1} - D_2 (\Lambda_1 + 1)) \|\tilde{\zeta} + \Gamma \tilde{\varphi}\|_0^2 + \frac{1}{E} (C_0 \Lambda^{-1} - D_2 \Lambda_1) \|\bar{\zeta} + \Lambda \bar{\varphi}\|_0^2. \end{aligned}$$

The last inequality uses the Poincaré inequality and the lower bound of the Dirichlet quotient  $\Lambda(t) \geq \Lambda_1$  derived before. The right hand side above may still reach positive values during the evolution of the system. Thus it is difficult in general to get the selective decay principle. Still, we can find one sufficient condition to guarantee selective decay in the combined effects of Landau damping and linear viscosity, that is,

$$C_0 \leq D_2 \Lambda_1^2.$$

The above relation makes sure that the right hand side of the dynamical equation is always negative in time. Then the monotonic decay of  $\Lambda(t)$  gets maintained. With larger values of  $C_0$ , however, the energy in the small scales may grow in time, thus may lead the the violation of the selective decay principle.

At last, to generalize from the previous special damping cases, a general dissipation form to guarantee the monotonic decrease of the Dirichlet quotient  $\Lambda(t)$  can be constructed to satisfy the following structure

$$\mathcal{D}(\Delta)\varphi = -\sum_{j=2}^L D_j \left[ (-\Delta + 1)^j \tilde{\varphi} + (-\partial_x^2)^j \bar{\varphi} \right] + D_1 (\Delta\varphi - \tilde{\varphi}). \quad (5.14)$$

We have shown that the second term above with  $D_1$  will not change the value of  $\Lambda(t)$ . The separated damping operators for the fluctuation  $\tilde{\varphi}$  and zonal state  $\bar{\varphi}$  are also reasonable considering the different treatment of the zonal state and fluctuations in the MHM equation. With detailed calculations, we show in Appendix A the explicit dynamical equation for  $\Lambda(t)$  under this generalized damping and its strictly decreasing features. To summarize, we use the following proposition to list all the results we achieved for the dynamics of the Dirichlet quotient:

**Proposition 3.** *The Dirichlet quotient  $\Lambda(t) = \frac{W(t)}{E(t)}$  is monotonically decreasing under the general damping form (5.14) as a combination of different orders of the Laplace operator on the zonal mean and fluctuation components. Specifically for several important special cases, we have:*

- i) *The leading order damping,  $D_1(\Delta\varphi - \tilde{\varphi})$ , will not alter the value of the Dirichlet quotient with conservation equation (5.9) for any values of the strength  $D_1$ . This term will act as an anti-damping effect to increase both energy and enstrophy with  $D_1 > 0$ ;*
- ii) *The second-order damping,  $-D_2(-\Delta q + \tilde{q})$ , guarantees the monotonic decrease of the Dirichlet quotient with the dynamical equation (5.11), while the first component of the damping only,  $D_2\Delta q$ , may violate the strictly decreasing property of  $\Lambda(t)$ ;*
- iii) *The ion Landau damping,  $C_0\varphi$ , increases the value of the Dirichlet quotient. As a result, it plays the role of transferring the energy downscale to generate more smaller-scale structures. In a combination with the second-order damping, the monotonic decrease of  $\Lambda(t)$  is resumed when the Landau damping strength becomes small enough,  $C_0 \leq D_2\Lambda_1^2$ .*

### 5.3 The convergence to the selective decay state

In the previous discussions, we have shown the convergence of the Dirichlet quotient  $\Lambda(t)$  in time with selective decay guaranteed damping operators. With the valid damping forms, the function  $\Lambda(t)$  is a monotonic decreasing function with a lower bound. Thus, we have the convergence for the quotient  $\Lambda(t)$  to a limit  $\Lambda_*$  as time goes to infinity

$$\lim_{t \rightarrow \infty} \Lambda(t) = \Lambda_* \geq \Lambda_1. \quad (5.15)$$

Here the next task is to show that the limit  $\Lambda_*$  can only be one of the eigenvalues (4.7) of the system. For the CHM model, the conclusion is directly from the convergence of the corresponding damping terms [13]. However, here for the MHM model, additional complexity appears due to the separation of the zonal state and fluctuations for separate treatment in the equation.

For simplicity, we consider only the second-order damping form (or assume there exists a non-zero second-order damping  $D_2$ )

$$\mathcal{D}(\Delta)\varphi = -D_2(-\Delta q + \tilde{q}).$$

The dynamical equation for the Dirichlet quotient  $\Lambda(t)$  in this case from (5.11) is

$$\frac{d\Lambda}{dt} = -\frac{D_2}{E} \left( \left\| \nabla \tilde{\zeta} + \Gamma \nabla \tilde{\varphi} \right\|_0^2 + \left\| \partial_x \bar{\zeta} + \Lambda \partial_x \bar{\varphi} \right\|_0^2 + \left\| \tilde{\zeta} + \Gamma \tilde{\varphi} \right\|_0^2 \right).$$

Integrating the above equation directly in time and letting  $t \rightarrow \infty$  gives the following relation with  $\Lambda(t) = \Gamma(t) + 1$

$$\int_0^\infty \frac{\left\| \tilde{\zeta} + \Gamma \tilde{\varphi} \right\|_0^2 + \left\| \nabla \tilde{\zeta} + \Gamma \nabla \tilde{\varphi} \right\|_0^2 + \left\| \partial_x \bar{\zeta} + \Lambda \partial_x \bar{\varphi} \right\|_0^2}{\left\| \nabla \tilde{\varphi} \right\|_0^2 + \left\| \tilde{\varphi} \right\|_0^2 + \left\| \partial_x \bar{\varphi} \right\|_0^2} dt \leq D_2^{-1} (\Lambda(0) - \Lambda_*) < \infty.$$

On the right hand side, strictly we have  $\Lambda(0) > \Lambda(t) > \Lambda_*$  at time  $0 < t < \infty$ . The finite value of the infinite integration on the left side requires the integrant to vanish as  $t \rightarrow \infty$ . Writing the integrant under each Fourier mode with eigenvalue  $\Lambda_k = (2\pi/L)^2 k^2$  gives

$$\begin{aligned} \frac{\left\| \tilde{\zeta} + \Gamma \tilde{\varphi} \right\|_0^2 + \left\| \nabla \tilde{\zeta} + \Gamma \nabla \tilde{\varphi} \right\|_0^2 + \left\| \partial_x \tilde{\zeta} + \Lambda \partial_x \tilde{\varphi} \right\|_0^2}{\left\| \nabla \tilde{\varphi} \right\|_0^2 + \left\| \tilde{\varphi} \right\|_0^2 + \left\| \partial_x \tilde{\varphi} \right\|_0^2} &= \frac{\sum_k (\Lambda_k - \Gamma(t))^2 (\Lambda_k + 1) |\tilde{\varphi}_k|^2 + \sum_l \Lambda_l (\Lambda_l - \Lambda(t))^2 |\tilde{\varphi}_l|^2}{\sum_k (\Lambda_k + 1) |\tilde{\varphi}_k|^2 + \sum_l \Lambda_l |\tilde{\varphi}_l|^2} \\ &\geq \min \left\{ \min_{k_x, k_y} |\Lambda_k - \Gamma(t)|^2, \min_l |\Lambda_l - \Lambda(t)|^2 \right\} \rightarrow 0, \end{aligned}$$

as  $t \rightarrow \infty$ , where  $\tilde{\varphi}_k$  is the fluctuation Fourier mode with  $k_y \neq 0$  and  $\tilde{\varphi}_l$  is the zonal Fourier mode with  $k_x = l$  and  $k_y = 0$ . Directly, we get that at least one of the two coefficients

$$\min_{k_x, k_y} |\Lambda_k + 1 - \Lambda(t)|, \text{ or } \min_l |\Lambda_l - \Lambda(t)|,$$

must go to zero at the long time limit. Then applying the above relation again for the other coefficient, we reach that both the coefficients must converge to zero as  $t$  goes to infinity. With the convergence of  $\Lambda(t)$  to a single eigenvalue, the final task is to show that  $\varphi(t)$  indeed converges to the corresponding selective decay eigenstate in  $H^1$  sense. The argument for the convergence is exactly same as in the CHM model case thus we neglect the details here. Detailed proofs are shown in [13] and [12] from two different approaches.

### 5.3.1 Two types of metastable or selective decay states

We have two types of final converged state  $\Lambda_k + 1$  and  $\Lambda_l$  for the state solution. In the first case, if  $\Lambda(t) \rightarrow \Lambda_k + 1 > 1$ , there exist non-zero fluctuation modes in the final selective decay state. On the other hand, there exists another possibility in the MHM model for the fluctuation modes to vanish uniformly,  $\tilde{\varphi} \equiv 0$ . If we have the quotient goes to some value smaller than 1,  $\Lambda(t) \rightarrow \Lambda_l < 1$ , the selective decay state is purely zonal. Then the ratio of the fluctuation modes must go to zero. In fact, if we have a series of  $\{t_j\}_{j=1}^\infty$ , so that the fluctuation modes are always non-vanishing at some wavenumber  $|\tilde{\varphi}_k(t_j)|^2 / E(t_j) \geq \delta > 0$ , then from the above relation for large enough time  $t > T$ , there always exists a sub-sequence (without loss of generality still represented as  $\{t_j\}$ ) so that

$$\frac{\sum_k (\Lambda_k - \Gamma(t_j))^2 (\Lambda_k + 1) |\tilde{\varphi}_k|^2(t_j) + \epsilon}{E(t_j)} > \frac{(\Lambda_k + 1 - \Lambda_*)^2 (\Lambda_k + 1) |\tilde{\varphi}_k|^2(t_j)}{E(t_j)} \geq c\delta > 0.$$

This violates the integrability of the above infinite integral. Therefore, we have the conclusion that if  $\Lambda_* < 1$ , the ratio of energy in the fluctuation modes must vanish in the large time limit, that is,

$$\frac{\tilde{E}(t)}{E(t)} \xrightarrow{t \rightarrow \infty} 0, \text{ when } \Lambda(t) \rightarrow \Lambda_* < 1.$$

Notice that the above argument dose not require the decaying property of the total energy  $E(t)$  or enstrophy  $W(t)$ . Then the conclusion is also valid for the generalized damping case in (2.2) where there exist anti-damping effects with  $D_1 > 0$  even to increase the energy and enstrophy. From another approach, we can also directly show from the dynamical equations of  $\bar{E}(t)$  and  $\tilde{E}(t)$  that the ratio  $\tilde{E}/E$  goes to zero at large time limit once the value of  $\Lambda(t)$  goes below 1. The detailed calculation is shown in Appendix C.

As a major difference from the original CHM model results, the conclusion for the final selective decay state in the MHM model emphasizes the role of the zonal state depending on the convergence value of the Dirichlet quotient  $\Lambda_*$ . We need to separately consider the two cases corresponding to the two sets of eigenfuctions found in (4.8) and (4.9), depending on whether all the fluctuation modes  $|\tilde{\varphi}_k|^2(t)/E(t)$  go to zero or not at the limit. In a similar way, we can determine the selective decay state in the following two cases. The result can be first summarized in the following theorem:

**Corollary 4.** *(selective decay state in the MHM model) There exist two types of admissible selective decay or metastable states in the MHM model with periodic boundary condition:*

- If there exists non-zero fluctuation component  $\tilde{\varphi}$  in the critical state, then the selective decay state is on a fixed energy shell with some eigenmode  $k$

$$\lim_{t \rightarrow \infty} \Lambda(t) = \Lambda_k + 1, \quad \Lambda_k = \left(\frac{2\pi}{L}\right)^2 k^2,$$

with the corresponding eigenfunction (4.8). Notice that the zonal mean mode  $\bar{\varphi} = A \cos \sqrt{\Lambda} x$  has the wavenumber always larger than 1 due to the above eigenvalue relation. This is usually the transient metastable state during the evolution of the solution.

- If there is no fluctuation component in the critical state, the system converges to a single zonal mode with wavenumber  $l$

$$\lim_{t \rightarrow \infty} \Lambda(t) = \left(\frac{2\pi}{L}\right)^2 l^2, \quad l \in \mathbb{N},$$

with the corresponding eigenfunction (4.9). The single zonal mode  $\bar{\varphi}_l$  can have any integer wavenumber  $l$ . Especially, if the final limit  $\Lambda_* < 1$ , the ratio of energy in the fluctuation modes,  $\tilde{E}/E$ , must converge to zero at the large time limit, and this is the final selective decay state the solution converges to.

The constraint in the zonal mode in the first case is due to the relation with a non-zero fluctuation mode, while in the second case without a fluctuation component, the zonal state can converge to any acceptable zonal mode. Still, the contribution from the non-zonal fluctuation perturbation should be considered. It is found that the stable zonal mode usually takes the wavenumber near the ground state  $\sqrt{\Lambda_1 + 1}$  due to the direct cascade of energy from this mode.

### 5.3.2 The stability of the zonal selective decay states

The last thing we need to show is the stability of the zonal modes. It can be seen first that the quotient in the fluctuation part

$$\tilde{\Lambda} = \frac{\|\Delta \tilde{\varphi} - \tilde{\varphi}\|^2}{\|\nabla \tilde{\varphi}\|^2 + \|\tilde{\varphi}\|^2} \geq \Lambda_1 + 1,$$

is always larger than one if there exists non-zero fluctuation. Then a perturbation in the zonal mode with  $\bar{\Lambda} < 1$  will always lead to a drop in value of the total quotient  $\Lambda(t)$ . Thus it shows that the first type of selective decay state with non-zero fluctuation mode with  $k_y \neq 0$  is unstable. The solution usually lingers around these metastable states for some time, and will finally go on decaying to a purely zonal state (Section 6.1 will show the numerical confirmation of such dynamical activities). Another way to understand the instability in the fluctuation mode is from the secondary instability [24], where the energy in drift waves keeps transferring to the large-scale zonal modes due to the nonlinear interactions.

To illustrate the result, consider a fluctuation mode  $\tilde{\varphi}_k$  on the energy shell  $\Lambda_k$ , so that,

$$\Lambda(\tilde{\varphi}_k) = \frac{(\Lambda_k + 1)^2 \|\tilde{\varphi}_k\|^2}{(\Lambda_k + 1) \|\tilde{\varphi}_k\|^2} = \Lambda_k + 1.$$

Then we introduce a small perturbation in the zonal mode  $\epsilon \bar{\varphi}_l$  with the eigenvalue smaller than one,  $\Lambda_l < 1$ . The Dirichlet quotient for the new perturbed variable  $\varphi = \tilde{\varphi}_k + \bar{\varphi}_l$  becomes

$$\Lambda(\varphi) = \frac{(\Lambda_k + 1)^2 \|\tilde{\varphi}_k\|^2 + \epsilon^2 \Lambda_l^2 \|\bar{\varphi}_l\|^2}{(\Lambda_k + 1) \|\tilde{\varphi}_k\|^2 + \epsilon^2 \Lambda_l \|\bar{\varphi}_l\|^2} = (\Lambda_k + 1) + \epsilon^2 \frac{\Lambda_l \|\bar{\varphi}_l\|^2}{E(\varphi)} (\Lambda_l - \Lambda_k - 1) < \Lambda_k + 1.$$

This shows that any eigenvalue  $\Lambda = \Lambda_k + 1$  larger than one will be reduced by introducing perturbations with zonal wavenumber smaller than one,  $\Lambda_l = \left(\frac{2\pi l}{L}\right)^2 < 1$ . Then the original selective decay state related with eigenvalue  $\Lambda_k + 1$  including non-zero fluctuation components becomes unstable and decays to the next state on the lower energy shell due to the strict monotonic decreasing property. Combining this with the previous conclusion in Corollary 4 that the only permitted selective decay states are associated with eigenvalue  $\Lambda_k + 1$  or  $\Lambda_l$ . This implies that the final stable eigenstate will always reach the purely zonal state with the corresponding eigenvalue  $\Lambda_* = \Lambda_l < 1$ . Then we have the following conclusion as a corollary:

**Corollary 5.** (*Stability of the selective decay states in the MHM model*) All the critical point states with a non-zero fluctuation component and eigenvalue  $\Lambda = \Lambda_k + 1$  in the MHM are unstable due to the arbitrary small zonal mode perturbations with eigenvalue  $\Lambda_l < 1$ . Then the solution of the MHM model usually visits several of these transient metastable critical states during its evolution in time, and will final go to the zonal selective decay state on a lower energy shell and contain only a zonal mode.

*Remark.* (the number of zonal jets in the final selective decay state) The result above still dose not tell which final zonal eigenstate  $\Lambda_l$  the system will actually converge to in the time limit. Practically, as we observe from various numerical simulations, the final zonal state is not always the state on the lowest energy shell (that is, with  $l = 1$ ) and is also related with the initial configuration. Usually, several intermediate saddle point solutions are generated at the same time depending on the initial configuration, then the lowest state with non-zero energy becomes the final selective decay solution that the system finally converges to.

## 6 Numerical Confirmation of the Selective Decay Principle

With the theoretical understanding about the MHM model, we present the selective decay and metastability properties through running direct numerical simulations. The equation (2.1) is solved on a doubly periodic domain. The variables of interest ( $\varphi, \zeta$ ) get the following spectral representations under Galerkin projection on the Fourier modes

$$\varphi = \sum_{|\mathbf{k}|=1}^N \hat{\varphi}_{\mathbf{k}}(t) e^{i\tilde{\mathbf{k}} \cdot \mathbf{x}}, \quad \zeta = \sum_{|\mathbf{k}|=1}^N -\tilde{k}^2 \hat{\varphi}_{\mathbf{k}}(t) e^{i\tilde{\mathbf{k}} \cdot \mathbf{x}},$$

with the spatial variables  $\mathbf{x} = (x, y)$  and the corresponding spectral wavenumbers

$$\tilde{\mathbf{k}} = \left( \frac{2\pi}{L_x} k_x, \frac{2\pi}{L_y} k_y \right), \quad (k_x, k_y) \in \mathbb{Z}^2.$$

In the numerical simulations, we assume the same length  $L_x = L_y = L$  along  $x$  and  $y$  directions. The lowest wavenumber becomes  $\Delta\tilde{k} = 2\pi/L$ , which is also the increment between two adjacent wavenumbers. A pseudo-spectral code with a 3/2-rule for de-aliasing the nonlinear term is applied on the square domain with length  $L = 40$  and resolution  $N = 256$ . A fourth-order explicit-implicit Runge-Kutta scheme is used to integrate the time steps. The background density gradient is fixed at  $\kappa = 0.5$ . The simulations are all run up to a large time much longer than the damping time scale. The model parameters are taken according to the more generalized numerical simulations in [11, 20].

For the dissipation operators, we majorly consider the following damping form

$$\mathcal{D}(\Delta) \varphi = -D_2 (-\Delta q + \tilde{q}) + C_0 \varphi. \quad (6.1)$$

As we have shown in the previous discussions, the first term with  $D_2$  guarantees the selective decay to a single mode zonal state, while the second term as the ion Landau damping  $C_0$  may lead to growth in small-scale fluctuations when  $C_0$  becomes large. We choose moderate viscosity  $D_2 = 1 \times 10^{-3}$ , and two different values of Landau damping  $C_0 = 0.01\kappa$  and  $C_0 = 0.05\kappa$  if added in the system. No extra forcing and hyperviscosity are added in the numerical scheme. The parameters for numerical simulations are summarized in Table 1.

We use the the initial profiles from [13] which are also tested for the CHM model (shown in Figure 3.1). The following three different initial states are considered in showing the system's decay from various starting structures:

- The initial states 1 and 2 use the form of the potential function first proposed from [21] where a broad spectrum is introduced by a superposition of many modes

$$\begin{aligned} \varphi_0 = & \cos(\alpha x + 0.3) + 0.9 \sin(3(\alpha y + 1.8) + 2\alpha x) \\ & + 0.87 \sin(4(\alpha x - 0.7) + (\alpha y + 0.4) + 0.815) \\ & + 0.8 \sin(5(\alpha x - 4.3) + 0.333) + 0.7 \sin(7\alpha x + 0.111). \end{aligned} \quad (6.2)$$

The parameter  $\alpha$  is used to control the smallest initial scale. The initial state 1 takes  $\alpha = \frac{\pi}{L}$  and the initial state 2 takes  $\alpha = \frac{2\pi}{L}$  with smaller-scale initial structures.

domain size $L$	40
spatial discretization $N$	256
time step $\Delta t$	$1 \times 10^{-3}$
mean density gradient $\kappa$	0.5
kinetic ion viscosity $D_2$	$1 \times 10^{-3}$
ion Landau damping $C_0$	0, 0.005, 0.025

Table 1: Basic model parameter values for numerical simulations.

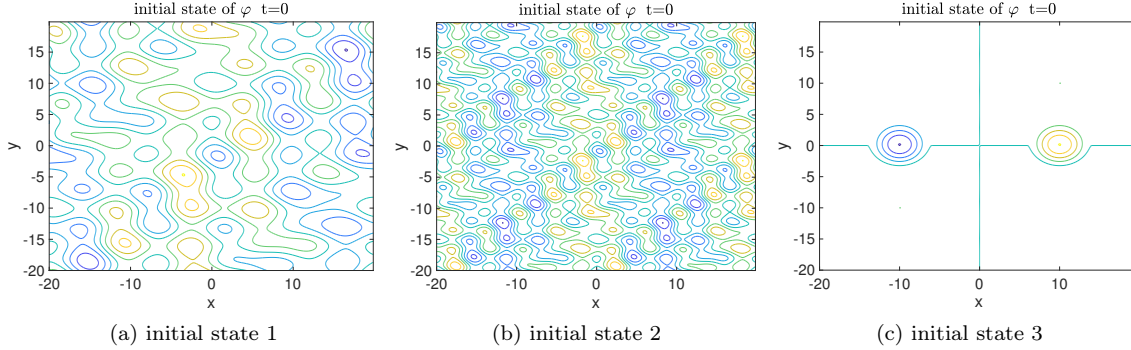


Figure 6.1: Snapshots of the initial states for the electrostatic potential function  $\varphi$ .

- The initial state 3 considers a large scale background mean solution adding small vortical fluctuations in the form

$$\varphi_0 = A_0 \sin\left(\frac{2\pi}{L_x}x\right) \sin\left(\frac{2\pi}{L_y}y\right) + \sum_{j=1}^2 A_j b_r(|\mathbf{x} - \mathbf{x}_j|), \quad (6.3)$$

where the two small vortices are aligned along  $x$ -axis with opposite signs

$$b_r(s) = \left| \max\left(0, 1 - \left(\frac{s}{r}\right)^2\right) \right|^2, \quad r = \frac{L}{20}, \quad \mathbf{x}_j = (\pm 10, 0).$$

The snapshots of the tested initial states are plotted in Figure 6.1. The first and second initial cases have the same structures but different scales controlled by the factor  $\alpha$ . We use this to check the selective decay state sensitivity to values in different initial state scales. In the third case, we set two vortices with opposite signs located on the  $x$ -axis. Thus they will be advected by the drift waves along  $y$ -direction while interact with each other.

## 6.1 Selective decay and metastability from different initial states

In the first test case, we monitor the selective decay performance with the damping operator  $-D_2(-\Delta q + \tilde{q})$ . From Theorem 2, the Dirichlet quotient  $\Lambda(t)$  will monotonically decrease to a final stable eigenvalue  $\Lambda_l < 1$  with a purely zonal single-mode solution. In the first column of Figure 6.2, we show the snapshots of the electrostatic potential function  $\varphi$  at the final simulation time starting from the three different initial states (6.2) and (6.3). Regardless of the distinct initial structures including much non-zonal fluctuations, the final solutions all converge to the purely zonal state without fluctuation modes under this selective decay guaranteed dissipation. Especially with the initial type 3 starting from two strong small vortices, the interacting vortices with opposite signs induce many multiscale structures in the transient states and then gradually break into larger scale structures.

One important observation from tracking the solution time evolution is the appearance of multiple time scales and many intermediate metastable states during the decaying process. Starting from the initial state, the flow solution usually first arrives at several intermediate saddle point states on higher energy levels before finally decays

to the stable purely zonal state. To characterize this, we introduce the normalized energy spectra in both the fluctuation modes and the zonal modes

$$\tilde{E}_k = \frac{k^2 |\tilde{\varphi}_k|^2}{\|\nabla\varphi\|_0^2}, \quad \bar{E}_l = \frac{l^2 |\bar{\varphi}_l|^2}{\|\nabla\varphi\|_0^2},$$

with  $\|\nabla\varphi\|_0^2 = \sum_k k^2 |\hat{\varphi}_k|^2$  the total kinetic energy. Above for the fluctuation modes  $(k_x, k_y)$  varying in the two-dimensional spectral space, we take the radial summation of all the modes  $k^2 = k_x^2 + k_y^2$  between two adjacent integer wavenumbers. In general, at the final time, the energy spectrum in fluctuations  $\tilde{E}_k$  becomes flat with uniform zero values, while the ratio of energy in the zonal modes  $\bar{E}_l$  goes to one at one single wavenumber and zero for all the other zonal modes.

The second parts of Figure 6.2 plot the normalized energy spectra  $\tilde{E}_k$  and  $\bar{E}_l$  at several intermediate time instants to illustrate the detailed decay process before it reaches the final zonal state. Starting from the different initial spectra, the solutions perform differently in the transient states, but always first visit several metastable intermediate states in (4.8) with eigenvalues larger than 1 and non-zero fluctuation modes. The solutions hover around these states for a while, and then break away from these unstable saddle point solutions and converge to the purely zonal final stable selective decay state in (4.9).

Specifically, in the first initial state, first two major fluctuation modes are generated on higher energy levels. Then the one with higher energy breaks down to create a single dominant fluctuation mode structure. Finally, all the energy in fluctuations decays to zero and a strong single zonal mode gradually forms up. In the second initial case with more smaller initial structures, the solution visits energy shells with even higher energy. There is a non-zero zonal mode with corresponding eigenvalue  $\Lambda > 1$ . Then this state becomes unstable, and the solution moves to the next intermediate energy level with lower energy. The energy in fluctuation keeps inversely cascading to larger scales and finally a single zonal mode forms up with eigenvalue  $\Lambda < 1$ . In contrast in the third initial state, there exists larger fluctuation energy among the largest scales at the starting time. But rapidly, the energy in fluctuation cascades downward to a smaller scales and creates both active zonal modes and fluctuations. Then the energy cascades inversely again and forms the final stable zonal selective decay solution. This case takes longer time to saturate due to the more complicated interactions.

As a final point, it is interesting to observe that the three initial cases give different numbers of zonal jets in the final selective decay states. Again it confirms that the final configuration is also related with the initial setup. Specifically here, it is related with the largest non-zero mode in the initial value. In the first two initial states, little energy is contained in the first few largest wavenumbers. Thus the final converged scale (with 5 or 4 jets) is determined by the lowest active wavenumber. In contrast, the third initial state gets larger energy in the largest scales at the initial time. Thus the energy in the lowest zonal wavenumber gets maintained and the system converges to the final solution in a larger scale with two zonal jets.

Next in Figure 6.3, the time evolutions of the the Dirichlet quotient  $\Lambda$ , total energy  $E$ , total enstrophy  $W$ , and anisotropic ratio  $\mathcal{R}$  are compared. With the dissipation form satisfying selective decay, the Dirichlet quotient  $\Lambda(t)$  decreases monotonically to the final limit  $0 < \Lambda_* < 1$  from all the three initial states. Notice that unlike the CHM case (shown in Figure 3.1),  $\Lambda(t)$  always goes below 1 implying that pure zonal structures are generated. For comparison, we also show the ratios in the zonal mean state only  $\bar{\Lambda}(t) = \frac{\bar{W}}{E}$ . Though the total ratio  $\Lambda(t)$  should always be monotonic, the quotient in the mean  $\bar{\Lambda}$  could either increase and decrease in the starting transient state.  $\bar{\Lambda}$  finally converges to the full Dirichlet quotient  $\Lambda$  at final time. Accordingly, the total energy and enstrophy also keep decreasing due to the pure damping effect without any forcing. Still the energy and enstrophy in the zonal mean part increase in the transient state and are approaching the total energy and enstrophy as time goes on. At last, as a measure for anisotropy, we compare the ratio

$$\mathcal{R} = \frac{\|\partial_x\varphi\|_0^2}{\|\nabla\varphi\|_0^2},$$

where the flow becomes purely zonal when  $\mathcal{R} = 1$ . In the selective decay cases, the ratios  $\mathcal{R}$  all approach 1, consistent with the theory and previous observations for the convergence to purely zonal structures. Besides, the final convergent state  $\Lambda_*$  and the time needed for the solution to reach the purely zonal flow depend on the initial states. Especially in the third initial state case with two interacting vortices, it takes much longer time for the small scale structures to be dissipated to reach the single dominant zonal mode.

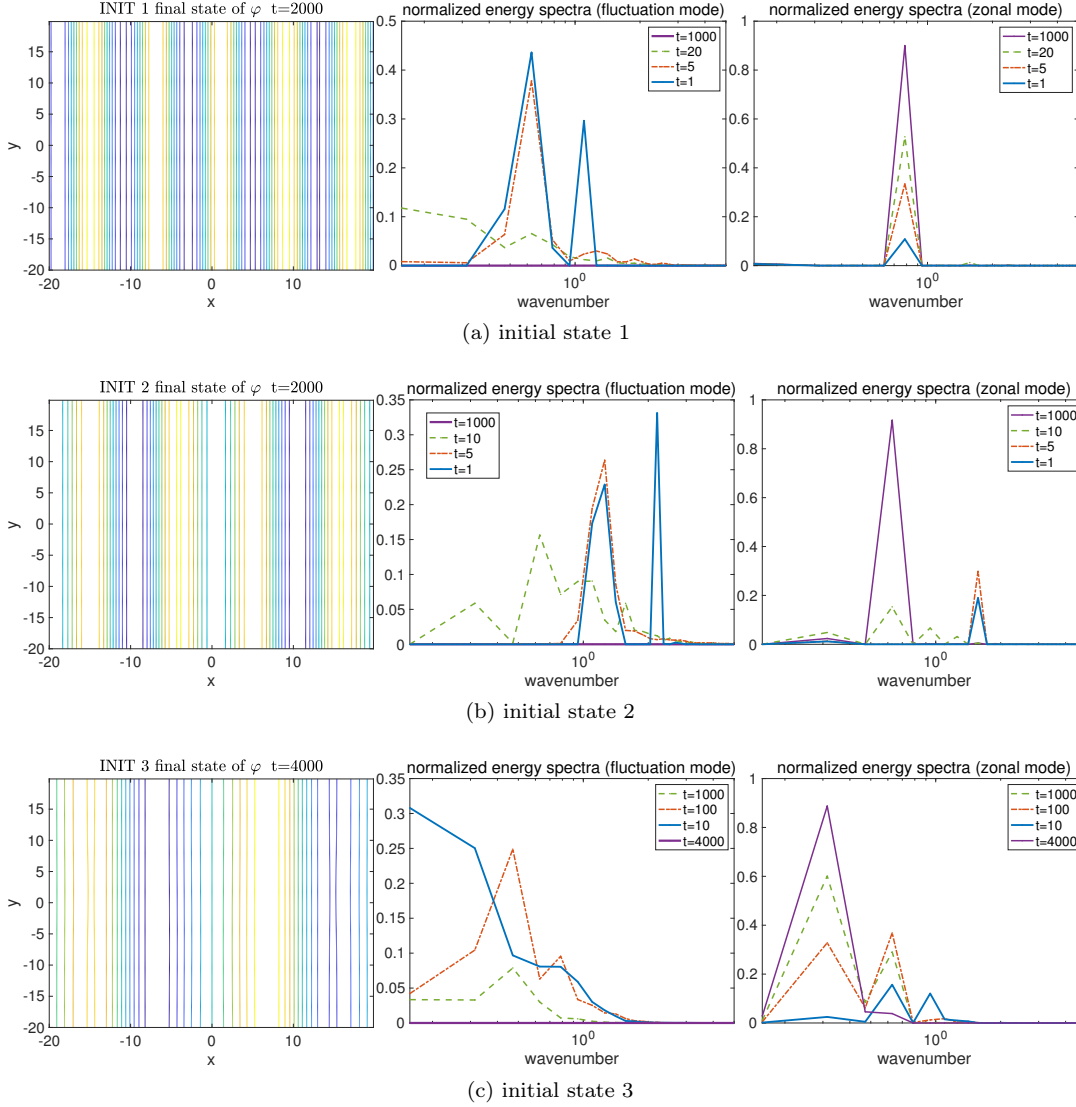


Figure 6.2: Snapshots of the electrostatic potential function  $\varphi$  with dissipation form  $-D(-\Delta q + \tilde{q})$  at the final simulation time, starting from three different initial states. The normalized energy spectra in both fluctuation modes  $k^2 |\tilde{\varphi}_k|^2 / \|\nabla \varphi\|_0^2$  (with  $k_y \neq 0$ ) and the zonal modes  $l^2 |\bar{\varphi}_l|^2 / \|\nabla \varphi\|_0^2$  are compared at different time instants. At the final time, the energy spectra in fluctuation modes always become flat with uniform zeros.

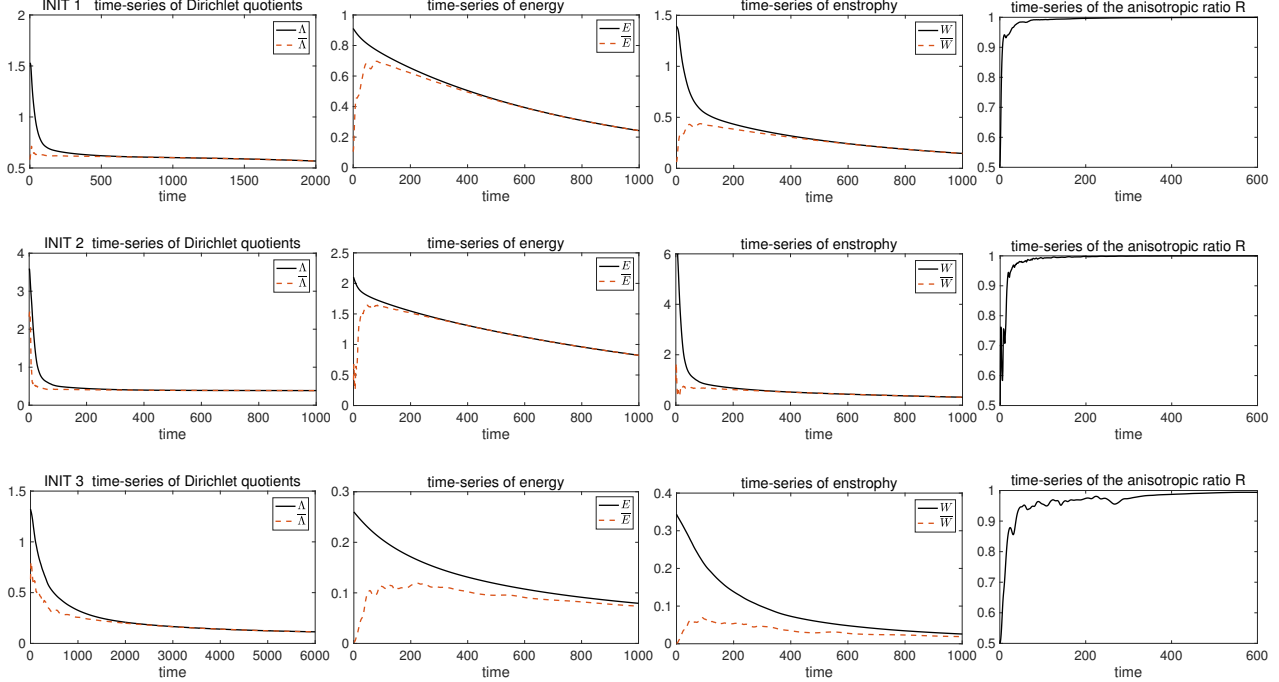


Figure 6.3: Time-series of the Dirichlet quotient  $\Lambda$ , total energy  $E$ , total enstrophy  $W$ , and anisotropic ratio  $\mathcal{R}$  from the three different types of initial states. The quantities only in the zonal modes are also compared in the first three plots.

## 6.2 The effect from the ion Landau damping

Next we add the effect of the ion Landau damping  $-D_2(-\Delta q + \tilde{q}) + C_0\varphi$  in addition to the previous damping form. As we have shown in the theoretical discussion, Landau damping with smaller strength can still maintain the selective decay principle, while when the Landau damping strength grows to larger values, more smaller scale modes get excited and destroy the original zonal selective decay state. In Figure 6.4, we first show the snapshots of the final potential function  $\varphi$  starting from initial state 1 with two different Landau damping strengths,  $C_0 = 0.005$  and  $C_0 = 0.025$ . The weaker Landau damping case still generates purely zonal flow in the final selective decay state with the same number of jets as the case without Landau damping (first row of Figure 6.2). In contrast, the strong Landau damping case keeps transporting energy to smaller scales, thus finally destroys the large-scale zonal structure.

We again plot the the normalized energy spectra in both fluctuation modes  $k^2 |\tilde{\varphi}_k|^2 / \|\nabla\varphi\|_0^2$  ( $k_y \neq 0$ ) and the zonal modes  $l^2 |\tilde{\varphi}_l|^2 / \|\nabla\varphi\|_0^2$  at different time instants for showing the detailed decaying process. In the weak Landau damping case, the decay from non-zonal modes to the final zonal selective decay state is observed in a similar way as the previous case without Landau damping. And the final zonal state has the same number of zonal jets. In the strong Landau damping case, in the starting transient states, we also observe the generation of several intermediate unstable selective decay states and the generation of a zonal state. However, due to the strong Landau damping in the largest scales, the zonal selective decay state is no longer persistent in this case. The energy begins to further move downscale. The portion of energy in the zonal state becomes negligible with only some modes in small scales remain in the final state. It shows the competition of two time scales: one for the generation of zonal selective decay state due to the original damping,  $-D_2(-\Delta q + \tilde{q})$ ; and the other for the downward cascade of energy due to the Landau damping,  $C_0\varphi$ .

In Figure 6.5, we plot the time-series of the Dirichlet quotient  $\Lambda$ , total energy  $E$ , total enstrophy  $W$ , and anisotropic ratio  $\mathcal{R}$  with the effect of Landau damping. The ratio  $\Lambda(t)$  is still monotonically decreasing in the weak Landau damping case, guaranteeing the selective decay principle in this case. For the case with strong Landau damping, the Dirichlet quotient  $\Lambda(t)$  is no longer monotonic and violates the selective decay. However in the starting time,  $\Lambda(t)$  still has a decreasing regime with the zonal structure developed from the more homogeneous

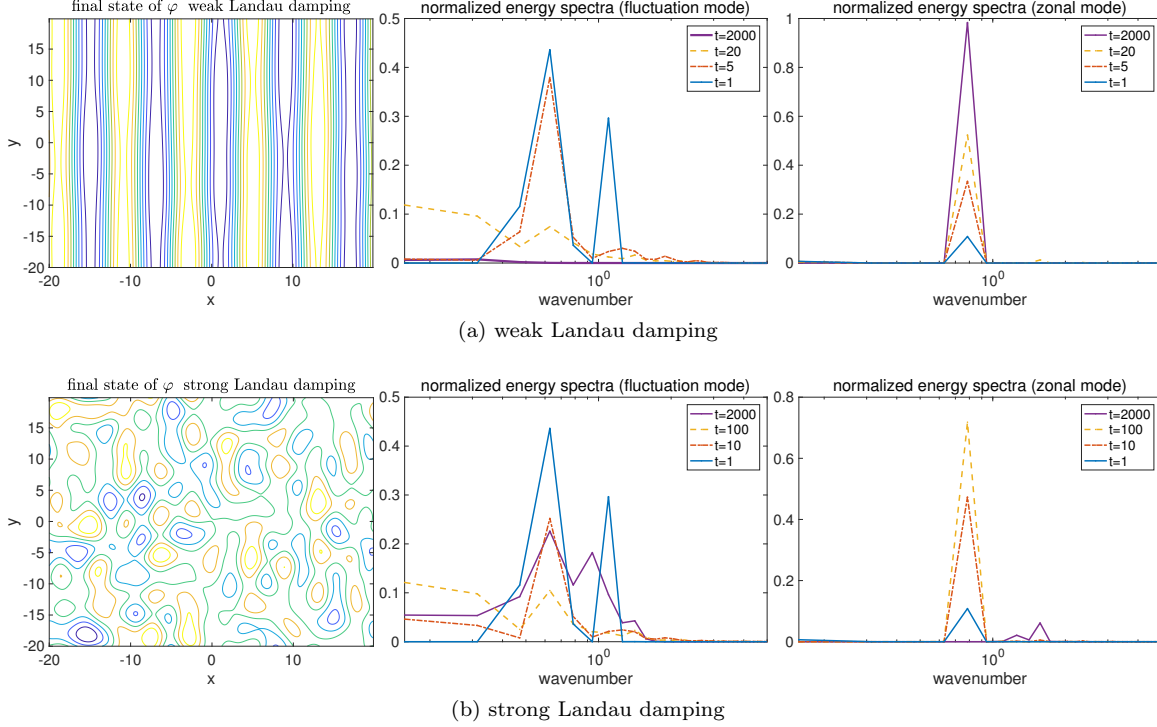


Figure 6.4: Snapshots of the electrostatic potential function  $\varphi$  at final time starting from initial state 1 with different Landau damping strengths  $C_0 = 0.005$  and  $C_0 = 0.025$ . The normalized energy spectra in both fluctuation modes  $k^2 |\tilde{\varphi}_k|^2 / \|\nabla\varphi\|_0^2$  and the zonal modes  $l^2 |\tilde{\varphi}_l|^2 / \|\nabla\varphi\|_0^2$  are compared at different time instants.

initial value. Then the Landau damping effect takes over to damp strongly on the large zonal scales and raise the portion of energy in the small-scale modes. The quotients in the zonal modes and fluctuations  $\bar{\Lambda}$  and  $\tilde{\Lambda}$  both increase in this case, showing the downscale cascade of energy in all modes. Both energy and enstrophy keep decreasing in a much faster rate compared with the previous cases due to the additional effect from Landau damping (especially for largest scales). The large-scale zonal structure is no longer persistent in time and also gets dissipated faster even in the weak Landau damping case due to the strong damping effect on the large scales.

### 6.3 Long-time phenomena with anti-damping effect: the large-scale condensation

In this final test case, we consider the large-scale energy condensation in one zonal mode with both damping and forcing effects in the MHM model. The forced-dissipated operator considered here has the form

$$\mathcal{D}(\Delta)\varphi = \mu(\Delta\varphi - \tilde{\varphi}) + D(\Delta^2\varphi - 2\Delta\tilde{\varphi} + \tilde{\varphi}), \quad (6.4)$$

on the right hand side of (2.1), with  $D > 0$  as the damping effect and  $\mu > 0$  as the forcing effect for the system. According to (2.7) and (2.8), the equations for energy  $E$  and enstrophy  $W$  according to this specific forcing and damping form (6.4) can be found as

$$\begin{aligned} \frac{dE}{dt} = & -D \left( \|\Delta\varphi\|_0^2 + 2\|\nabla\tilde{\varphi}\|_0^2 + \|\tilde{\varphi}\|_0^2 \right) \\ & + \mu \left( \|\nabla\varphi\|_0^2 + \|\tilde{\varphi}\|_0^2 \right); \end{aligned}$$

and

$$\begin{aligned} \frac{dW}{dt} = & -D \left( \|\Delta\nabla\varphi\|_0^2 + 2\|\Delta\tilde{\varphi}\|_0^2 + \|\nabla\tilde{\varphi}\|_0^2 \right) \\ & + \mu \left( \|\Delta\varphi\|_0^2 + 2\|\nabla\tilde{\varphi}\|_0^2 + \|\tilde{\varphi}\|_0^2 \right). \end{aligned}$$

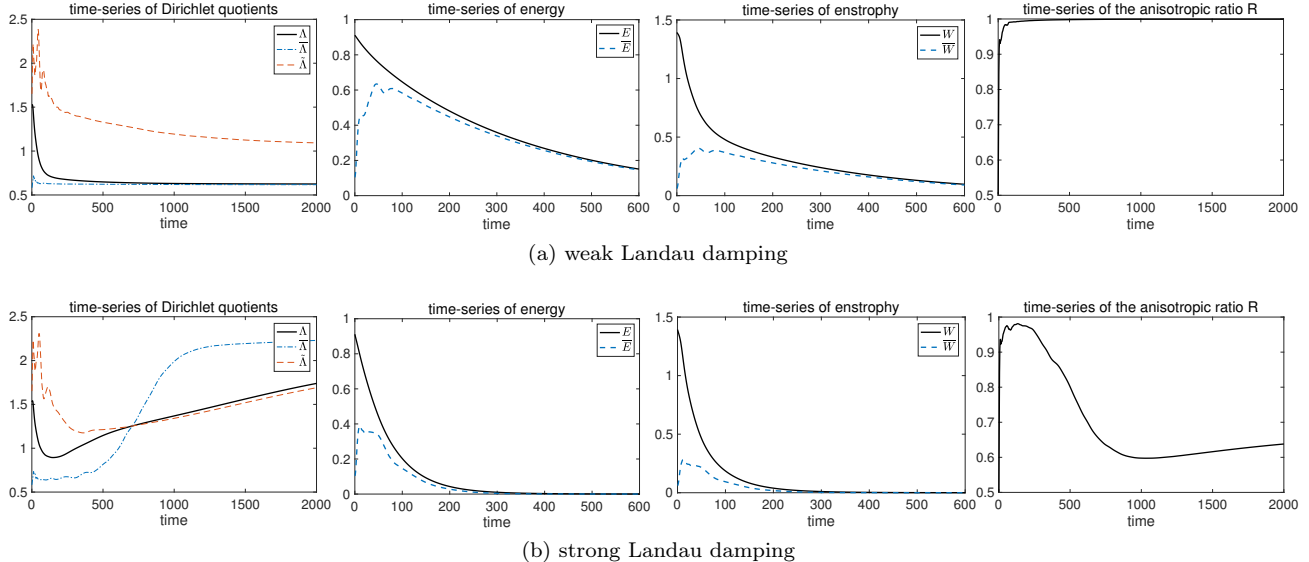


Figure 6.5: Time-series of the Dirichlet quotient  $\Lambda$ , total energy  $E$ , total enstrophy  $W$ , and anisotropic ratio  $\mathcal{R}$  with Landau damping. Results with different Landau damping strengths are displayed. The initial state 1 is used in the tests.

Therefore, both the energy and enstrophy may increase in time due to the forcing effect from the parameter  $\mu$ . This is no longer the exact selective decay case as in the previous tests since the amplitudes of the modes actually do not keep decreasing any more. Particularly, from the above energy and enstrophy equations, we observe that a saturated energy  $E_*$  and enstrophy  $W_*$  can be reached only if the potential function converges to the eigenmode  $\varphi_*$  on a single energy shell with corresponding eigenvalue  $\Lambda_*$ . This implies the constraints between the model parameters for a saturated state to be reached

$$D\Lambda_* = \mu,$$

with  $\Lambda_* = \left(\frac{2\pi}{L}\right)^2 k^2 + 1$  for non-zero fluctuation mode, and  $\Lambda_* = \left(\frac{2\pi}{L}l\right)^2$  for the purely zonal state. On the other hand, the permitted eigenvalue  $\Lambda_*$  may not usually agree with the above parameter constraint for a saturated steady state. This implies that the total energy and enstrophy may keep increasing from the combined forced-dissipated form (6.4).

On the other hand, the conclusion from Theorem 2 is still valid here under this forced-dissipated form since the effect from  $\mu$  does not change the value of the Dirichlet quotient  $\Lambda(t) = W(t)/E(t)$ , so that  $\Lambda(t)$  monotonically decreases to one eigenvalue  $\Lambda_*$  with

$$\Lambda_0 \geq \Lambda(t) \geq \Lambda_*$$

for all the time. Therefore, we can still expect a final purely zonal state with corresponding eigenvalue  $\Lambda_l$ . And the ratio of energy among all the other modes decreases to zero in time. At the same time, the forcing effect increases the total energy and enstrophy in the system. Then it implies that the single dominant mode will increase in energy in time, and all the energy will get condensed in this single mode.

Here in the numerical tests, we test three different values of the anti-damping parameter,  $\mu = 2 \times 10^4, 5 \times 10^{-4}, 1 \times 10^{-3}$ . Still we set the system to start from the initial state 1. In Figure 6.6, the first row shows the zonal mean profiles  $\bar{v} = \partial_x \bar{\varphi}$  with different parameter values of  $\mu$  at several different time instants. The system always reaches the final purely zonal state. With small  $\mu$ , the energy in the dominant zonal mode decreases in time similar as the previous selective decay case. As the value of  $\mu$  becomes larger, the final mean state stops decreasing, and finally begins to increase in amplitude with the largest values of  $\mu$ . In the second row, we further compare the energy in the large scale modes with  $k < 5$ , in the small scale modes with  $k > 5$ , and the single selected zonal mode with  $k = 5$ . In agreement with the theory, the energy among all the other modes decays in time regardless of the positive forcing, while the energy in the selective decay mode may either increase or decrease depending on the forcing strength  $\mu$ . Finally in the last row for checking the time evolution of the Dirichlet quotient  $\Lambda(t)$  as well as the energy and enstrophy,  $\Lambda(t)$  is still monotonically decreasing among all the cases with different forcing values

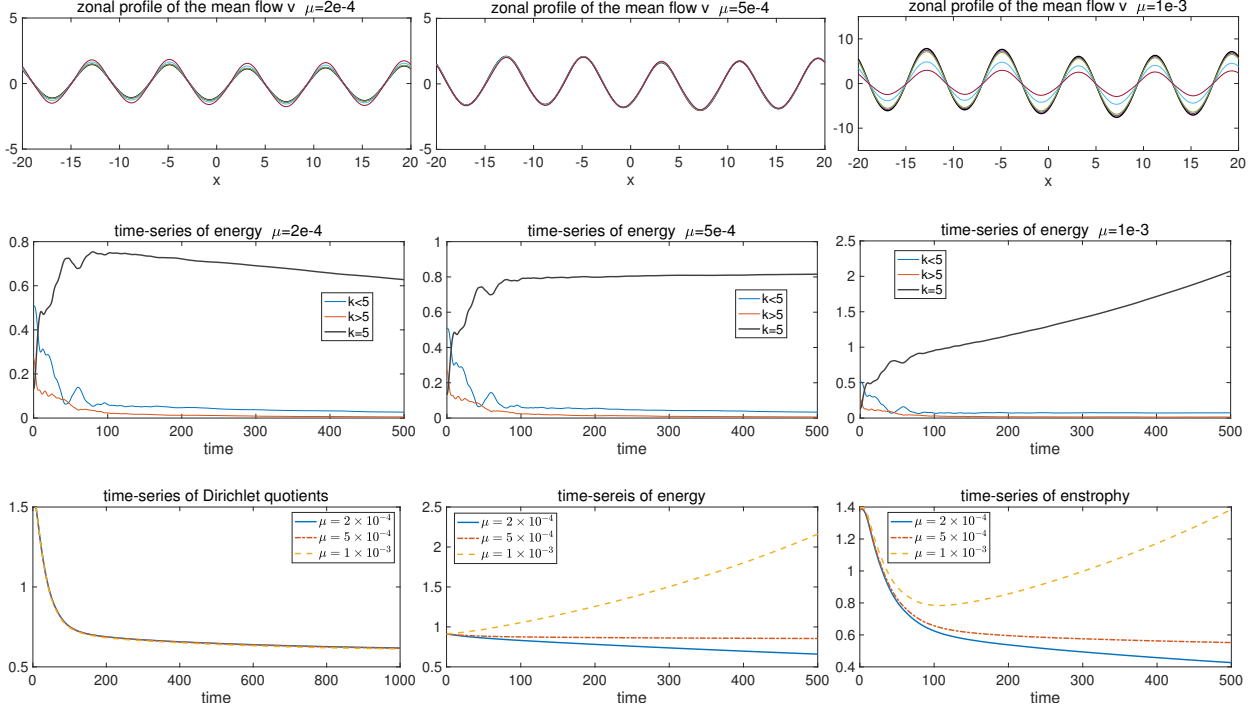


Figure 6.6: First line: the zonal mean flow  $v = \partial_x \bar{\varphi}$  with different values of the anti-damping parameter  $\mu = 2 \times 10^{-4}, 5 \times 10^{-4}, 1 \times 10^{-3}$  at several different time instants. The final state is plotted in thick black line. Second line: time-series of the energy in the large scale modes  $k < 5$ , the small scale modes  $k > 5$ , and the non-zero zonal mode  $k = 1$ . Third line: time-series of the Dirichlet quotient  $\Lambda$ , total energy  $E$ , total enstrophy  $W$ .

of  $\mu$ , confirming the single large-scale mode condensation from the theorem. In comparison, the total energy and enstrophy decrease in the smallest forcing case, but begin to grow in value as  $\mu$  increases to the largest value.

## 7 Summary

In this paper, we discussed the emergence of the coherent zonal structures in the freely decay plasma edge turbulence using the modified Hasegawa-Mima model. The argument follows the selective decay principle [13, 12] developed for the Charney-Hasegawa-Mima model (or equivalently the quasi-geostrophic model). In the investigation of the zonal flow generation, it is found that the MHM model with the particle response correction on magnetic surfaces can excite much stronger zonal mean flow than the classical CHM model [1, 11]. We first describe the outstanding zonal structures in the MHM model from the variational principle where the enstrophy reaches a critical point with constant energy. Then the general convergence to the purely zonal state is shown under the selective decay permitted dissipation forms. The argument depends on the dynamics of the Dirichlet quotient defined as the ratio between the total enstrophy and energy. Under proper generalized dissipation operators, the Dirichlet quotient monotonically converges to one of the eigenvalues of the critical states, implying the convergence of the flow solution to one selected state on a single energy shell. The special role of the zonal modes is further confirmed with the faster decay of energy in all the fluctuation modes. Then the zonal state becomes the only possible stable final selective decay state, while all the other critical point solutions act as transient metastable states which the solution visits during its time evolution before the final convergence.

Direct numerical simulations of the MHM model are used to confirm the final selective decay to zonal structures independent of various small-scale fluctuations introduced in the initial states. In particular, we investigated the effects from two terms usually with particular interests. The ion Landau damping strongly dissipates the largest scales and leads to forward energy transport to smaller scales. Then the selective decay to large-scale zonal flow will be destroyed when the Landau damping is dominant. In the second case, an anti-damping term that increases both energy and enstrophy is considered, while at the same time still guarantees the generation of a single zonal

mode. This creates a large-scale condensation inducing a single zonal state with increasing amplitude in time. The generation of zonal states is also related with the nonlinear instabilities and the nonlinear transfer of energy between the zonal states and non-zonal fluctuation modes [10, 24, 19]. One interesting direction in the next step is to consider the detailed energy mechanism in the high-order interactions between modes. In this way, the selective decay phenomena can be further understood with the internal instability and the external forcing.

## Acknowledgement

This research of the A. J. M. is partially supported by the Office of Naval Research through MURI N00014-16-1-2161 and DARPA through W911NF-15-1-0636. D. Q. is supported as a postdoctoral fellow on the second grant.

## A Generalized dissipation form with selective decay

In this appendix, we show the derivation for the general dissipation form that is in agreement with the selective decay principle. As from the main text for the proof of selective decay, the major task is to construct the proper damping operators  $\mathcal{D}(\Delta)$  on the right hand side of (5.3) so that the Dirichlet quotient  $\Lambda(t)$  stays monotonically decreasing in time. From the first and second order selective decay damping forms in Section 5.2, it can be summarized that the agreeable dissipation operators for selective decay should follow the general structure

$$\mathcal{D}(\Delta)\varphi = -\sum_{j=2}^L D_j \left[ (-\Delta + 1)^j \tilde{\varphi} + (-\partial_x^2)^j \bar{\varphi} \right] + D_1 (\Delta\varphi - \bar{\varphi}), \quad (\text{A.1})$$

with damping coefficients  $D_j \geq 0, j \geq 2$ . We have shown in (5.9) that the first order term above with any constant value  $D_1$  will not change the value of  $\Lambda(t)$  during its time evolution. The separated damping effects on the fluctuation  $\tilde{\varphi}$  and zonal mean  $\bar{\varphi}$  are reasonable considering the different treatment of the two parts in the MHM model. Next, we derive the dynamical equations for the Dirichlet quotient with a single order damping  $j$  from (A.1).

First from the equation (5.3), we have found the dynamical equations for  $\Lambda(t)$  subject to the damping with a single order of the Laplace operator applied on either the full potential function or its fluctuation part  $\tilde{\varphi} = \varphi - \bar{\varphi}$

$$\begin{aligned} \frac{d\Lambda}{dt} &= -\frac{d_j}{E} U_{j+1}, \quad \text{with } \mathcal{D}_j \varphi = d_j (-\Delta)^j \varphi, \\ \frac{d\Lambda}{dt} &= -\frac{d_j}{E} \tilde{U}_{j+1}, \quad \text{with } \tilde{\mathcal{D}}_j \varphi = d_j (-\Delta)^j \tilde{\varphi}. \end{aligned}$$

Then for the generalized damping form in (A.1), we can consider the effects componentwisely through the polynomial expansion of the damping operator

$$(-\Delta + 1)^j \tilde{\varphi} = \sum_{l=0}^j \lambda_l (-\Delta)^l \tilde{\varphi},$$

with the coefficients  $\lambda_l = \binom{j}{l}$ . Accordingly for the general damping of a single order  $j$ ,

$$-D_j \left[ (-\Delta + 1)^j \tilde{\varphi} + (-\partial_x^2)^j \bar{\varphi} \right] = -D_j \left[ (-\Delta)^j \varphi + \sum_{l=0}^{j-1} \lambda_l (-\Delta)^l \tilde{\varphi} \right],$$

we get the dynamical equation for  $\Lambda(t)$  in the expansion form by adding up all the component contributions as

$$\frac{d\Lambda}{dt} = -\frac{D_j}{E} \left( U_{j+1} + \sum_{l=0}^{j-1} \lambda_l \tilde{U}_{l+1} \right), \quad (\text{A.2})$$

where we use the notation  $U_j = \bar{U}_j + \tilde{U}_j$  from (5.4) for the contributions from the zonal mean and fluctuation components

$$\begin{aligned}\bar{U}_j &= \left\| (-\partial_x^2)^{\frac{j}{2}} \bar{\varphi} \right\|_0^2 - \Lambda(t) \left\| (-\partial_x^2)^{\frac{j-1}{2}} \bar{\varphi} \right\|_0^2, \\ \tilde{U}_j &= \left\| (-\Delta)^{\frac{j}{2}} \tilde{\varphi} \right\|_0^2 - \Gamma(t) \left\| (-\Delta)^{\frac{j-1}{2}} \tilde{\varphi} \right\|_0^2.\end{aligned}$$

Then the task is to reorganize the right hand side of (A.2) into a summation of non-positive quantities.

Next, we show the derivation of the recursive relations between the quantities defined in (5.4) and (5.6)

$$\tilde{U}_{j+1} = \tilde{S}_j + \Gamma \tilde{U}_j, \quad U_{j+1} = S_j + \Lambda \bar{U}_j + \Gamma \tilde{U}_j, \quad S_1 = -\Lambda U_1. \quad (\text{A.3})$$

The third relation is already derived in (5.5) directly from the definition of the Dirichlet quotient. The first two relations are the results from an integration by parts, that is, to get the fluctuation part

$$\begin{aligned}\tilde{U}_{j+1} &= \int \left| (-\Delta)^{\frac{j+1}{2}} \tilde{\varphi} \right|^2 - \Gamma \left| (-\Delta)^{\frac{j}{2}} \tilde{\varphi} \right|^2 \\ &= \int \left[ \left| (-\Delta)^{\frac{j+1}{2}} \tilde{\varphi} + \Gamma (-\Delta)^{\frac{j+1}{2}-1} \tilde{\varphi} \right|^2 - 2\Gamma \left( \nabla (-\Delta)^{\frac{j}{2}} \tilde{\varphi} \right) \left( (-\Delta)^{\frac{j}{2}-\frac{1}{2}} \tilde{\varphi} \right) \right. \\ &\quad \left. - \Gamma^2 \left| (-\Delta)^{\frac{j+1}{2}-1} \tilde{\varphi} \right|^2 - \Gamma \left| (-\Delta)^{\frac{j}{2}} \tilde{\varphi} \right|^2 \right] \\ &= \int \left| (-\Delta)^{\frac{j+1}{2}} \tilde{\varphi} + \Gamma (-\Delta)^{\frac{j+1}{2}-1} \tilde{\varphi} \right|^2 + \int \Gamma \left| (-\Delta)^{\frac{j}{2}} \tilde{\varphi} \right|^2 - \Gamma^2 \left| (-\Delta)^{\frac{j-1}{2}} \tilde{\varphi} \right|^2 \\ &= \int \left| (-\Delta)^{\frac{j+1}{2}} \tilde{\varphi} + \Gamma (-\Delta)^{\frac{j-1}{2}} \tilde{\varphi} \right|^2 + \Gamma \tilde{U}_j.\end{aligned}$$

Above in the second line, remind the notation  $(-\Delta)^{\frac{1}{2}} = \nabla$ , thus integration by parts can be applied for the second term. In a similar fashion, we can find the relation in the zonal mean modes by applying the same trick. Therefore, by introducing the definition for the positive-definite components,

$$\tilde{S}_j = \left\| (-\Delta)^{\frac{j+1}{2}} \tilde{\varphi} - \Gamma (-\Delta)^{\frac{j-1}{2}} \tilde{\varphi} \right\|_0^2, \quad \bar{S}_j = \left\| (-\partial_x^2)^{\frac{j+1}{2}} \bar{\varphi} - \Lambda (-\partial_x^2)^{\frac{j-1}{2}} \bar{\varphi} \right\|_0^2,$$

the above two identities are reached. Notice that we have different coefficients  $\Lambda(t) = \Gamma(t) + 1$  in the zonal mean and fluctuation parts.

Now we can derive the final form of the dynamics of (A.2) by applying the identities (A.3) recursively from the original equation. The leading term  $U_{j+1}$  can be expanded into all the lower order terms

$$\begin{aligned}U_{j+1} &= S_j + \sum_{l=1}^{j-1} \left( \Gamma^{j-l} \tilde{S}_l + \Lambda^{j-l} \bar{S}_l \right) + \Lambda^j U_1 + \Gamma^j \tilde{U}_1 - \Lambda^j \tilde{U}_1 \\ &= S_j + \sum_{l=1}^{j-1} \left( \Gamma^{j-l} \tilde{S}_l + \Lambda^{j-l} \bar{S}_l \right) - \Lambda^{j-1} S_1 + \Gamma^j \tilde{U}_1 - \Lambda^j \tilde{U}_1 \\ &= S_j + \sum_{l=2}^{j-1} \left( \Gamma^{j-l} \tilde{S}_l + \Lambda^{j-l} \bar{S}_l \right) + (\Gamma^{j-1} - \Lambda^{j-1}) \tilde{S}_1 + (\Gamma^j - \Lambda^j) \tilde{U}_1.\end{aligned}$$

We only need to attend to the last non-definite term above. Again we can expand the coefficient in the polynomial form and notice  $\lambda_j = 1$

$$(\Gamma^j - \Lambda^j) \tilde{U}_1 = \left[ \Gamma^j - (1 + \Gamma)^j \right] \tilde{U}_1 = - \sum_{l=0}^{j-1} \lambda_l \Gamma^l \tilde{U}_1.$$

For each component of the above summation with index  $l$ , using the relation  $\tilde{U}_{j+1} = \tilde{S}_j + \Gamma\tilde{U}_j$  inversely, we find the further expansion

$$\begin{aligned} -\lambda_l \Gamma^l \tilde{U}_1 &= \lambda_l \Gamma^{l-1} (\tilde{S}_1 - \tilde{U}_2) \\ &= \lambda_l \Gamma^{l-1} \tilde{S}_1 + \lambda_l \Gamma^{l-2} (\tilde{S}_2 - \tilde{U}_3) \\ &= \lambda_l \sum_{i=1}^l \Gamma^{l-i} \tilde{S}_i - \lambda_l \tilde{U}_{l+1}. \end{aligned}$$

Therefore, by taking the summation of all the components we get

$$-\sum_{l=0}^{j-1} \lambda_l \Gamma^l \tilde{U}_1 = \sum_{l=1}^{j-1} \lambda_l \sum_{i=1}^l \Gamma^{l-i} \tilde{S}_i - \sum_{l=0}^{j-1} \lambda_l \tilde{U}_{l+1}.$$

Again the first part above is positive definite, and the second part then can be exactly cancelled by the rest terms in the full dynamics (A.2). Combining all the above results, we finally reach the form for the total damping contributions from the  $j$ -th order dissipation operator

$$\begin{aligned} U_{j+1} + \sum_{l=0}^{j-1} \lambda_l \tilde{U}_{l+1} &= S_j + \sum_{l=2}^{j-1} (\Gamma^{j-l} \tilde{S}_l + \Lambda^{j-l} \bar{S}_l) + (\Gamma^{j-1} - \Lambda^{j-1}) \tilde{S}_1 + \sum_{i=1}^{j-1} \Gamma^{-i} \tilde{S}_i \sum_{l=i}^{j-1} \lambda_l \Gamma^l \\ &= S_j + \sum_{l=2}^{j-1} (\Gamma^{j-l} \tilde{S}_l + \Lambda^{j-l} \bar{S}_l) + (\Lambda^{j-1} - 1) \Gamma^{-1} \tilde{S}_1 + \sum_{i=2}^{j-1} \Gamma^{-i} \tilde{S}_i \sum_{l=i}^{j-1} \lambda_l \Gamma^l. \end{aligned}$$

Above in the first line, we just change the order of summation for the last term, and notice that the first term in the summation with  $i = 1$  in the last summation can be combined with the second term with  $\tilde{S}_1$ , that is,

$$\Gamma^{-1} \tilde{S}_1 \sum_{l=1}^{j-1} \lambda_l \Gamma^l = \Gamma^{-1} \tilde{S}_1 \left( \sum_{l=0}^j \lambda_l \Gamma^l - \Gamma^j - 1 \right) = (1 + \Gamma)^j \Gamma^{-1} \tilde{S}_1 - (\Gamma^{j-1} + \Gamma^{-1}) \tilde{S}_1,$$

and combining the coefficients

$$(\Gamma^{j-1} - \Lambda^{j-1}) + \Gamma^{-1} \sum_{l=1}^{j-1} \lambda_l \Gamma^l = \Lambda^j \Gamma^{-1} - \Lambda^{j-1} - \Gamma^{-1} = \Lambda^{j-1} \Gamma^{-1} - \Gamma^{-1}.$$

In summary, the final dynamical equation for the Dirichlet quotient  $\Lambda(t)$  under the general  $j$ -th order ( $j > 1$ ) damping operator in (A.1) can be found to satisfy the following form

$$\frac{d\Lambda}{dt} = -\frac{D_j}{E} \left[ S_j + \sum_{l=2}^{j-1} \left( \Lambda^{j-l} \bar{S}_l + \sum_{i=l}^j \lambda_i \Gamma^{i-l} \tilde{S}_i \right) + (\Lambda^{j-1} - 1) \Gamma^{-1} \tilde{S}_1 \right], \quad (\text{A.4})$$

with  $\Lambda = \Gamma + 1$  and  $\lambda_l = \binom{j}{l}$  the coefficients before the  $x^l$  term in the polynomial expansion of  $(x+1)^j$ . The right hand side of the above equation is always non-positive. Therefore, we conclude that  $\Lambda(t)$  is a monotonically decreasing function in time with a lower bound. The same selective decay principle still applies in the general case.

## B A counter-example that violates the selective decay

We have shown in Section 5.2 of the main text that the damping form,  $D(\Delta q - \tilde{q})$ , gives the convergence to the selective decay state. The second part in the damping form  $-D\tilde{q}$  includes a pure effect on the fluctuations. Here as a counter example, we show the second component is essential in maintaining the monotonically decreasing property of the Dirichlet quotient in the MHM model.

For the case with only damping on the potential vorticity

$$\mathcal{D}\varphi = D\Delta q = D(\Delta^2\varphi - \Delta\tilde{\varphi}),$$

the dynamical equation for the Dirichlet quotient becomes

$$\begin{aligned} \frac{d\Lambda}{dt} = & -D \left( \left\| \nabla \tilde{\zeta} + \Gamma \nabla \tilde{\varphi} \right\|_0^2 + \left\| \partial_x \bar{\zeta} + \Lambda \partial_x \bar{\varphi} \right\|_0^2 \right) \\ & + D\Lambda \left( \left\| \nabla \tilde{\varphi} \right\|_0^2 - \Gamma \left\| \tilde{\varphi} \right\|_0^2 \right). \end{aligned} \quad (\text{B.1})$$

Without the zonal state  $\bar{\varphi} \equiv 0$ , it can be seen from Poincaré inequality that the right hand side of (B.1) is still non-positive definite just as the CHM case. However, with the effect of a non-zero zonal flow, the term on the second line above is indefinite about its sign. The last indefinite term reflects the interactions between the fluctuation and zonal mean state through the entire Dirichlet quotient  $\Lambda(t)$  that includes ratios of both mean and fluctuation parts. Without the detailed dynamics, it is hard to determine the energy transfer mechanism between the zonal mean and the fluctuation. To show this, consider a small non-zonal perturbation added on a zonal solution

$$\varphi_0 = A \cos \sqrt{\Lambda_l + 1} x + \epsilon \cos \left( \frac{2\pi}{L} \mathbf{k} \cdot \mathbf{x} \right),$$

with  $\Lambda_l = \left( \frac{2\pi}{L} l \right)^2$ ,  $\Lambda_k = \left( \frac{2\pi}{L} k \right)^2$ ,  $k > l$  and  $\epsilon^2 < A^2$ . Then we can calculate the Dirichlet quotient for this initial state as

$$\Lambda_l + 1 < \Lambda(0) = \frac{(\Lambda_k + 1)^2 \epsilon^2 + (\Lambda_l + 1)^2 A^2}{(\Lambda_k + 1) \epsilon^2 + (\Lambda_l + 1) A^2} < \Lambda_k + 1.$$

Substituting the state into the right hand side of the equation (B.1), we have the estimation for the initial transient state dynamics with the state  $\varphi_0$

$$\begin{aligned} \frac{d\Lambda}{dt} & \geq -D \left[ \Lambda_k (\Lambda_k + 1 - \Lambda(0))^2 \epsilon^2 + (\Lambda_l + 1) (\Lambda_l + 1 - \Lambda(0))^2 A^2 \right] \\ & \quad + D\Lambda(0) \frac{(\Lambda_l + 1) (\Lambda_k - \Lambda_l) A^2}{(\Lambda_k + 1) \epsilon^2 + (\Lambda_l + 1) A^2} \epsilon^2 \\ & \geq -D (\Lambda_k - \Lambda_l)^2 (\Lambda_k \epsilon^2 + (\Lambda_l + 1) A^2) + \frac{(\Lambda_l + 1)^2 (\Lambda_k - \Lambda_l)}{(\Lambda_k + 1) + (\Lambda_l + 1)} \epsilon^2. \end{aligned}$$

Therefore the right hand side of the equation is larger than zero if

$$\epsilon^2 > \frac{\left[ (\Lambda_k + 1)^2 - (\Lambda_l + 1)^2 \right] (\Lambda_l + 1)}{\left[ (\Lambda_l + 1)^2 - \Lambda_k (\Lambda_k + 1) \right] (\Lambda_k + 1)} A^2.$$

Then by taking the wavenumbers satisfying  $\Lambda_k (\Lambda_k + 1) < (\Lambda_l + 1)^2 < (\Lambda_k + 1)^2$ , the Dirichlet quotient will increase in the initial state. Inversely. The larger value of  $\Lambda(t)$  further implies the generation of more higher wavenumber fluctuation modes, thus to push the quotient to even larger values. As a result, this example with special initial state shows that the monotonic decrease of the Dirichlet quotient might be violated with the pure damping form  $D\Delta q$ . Then the selective decay principle is difficult to guarantee in this case.

## C Dynamical convergence to the zonal mean flow

For the convergence to a purely zonal state, we have proved in the main text using the convergence of the infinite integral in the dynamical equation of  $\Lambda(t)$ . Here as an alternative approach, we directly show the convergence to zero in the ratio of energy fluctuation from the dynamical equations for the mean and fluctuation parts.

We consider the convergence to a purely zonal state with the dissipation form  $-D_2(-\Delta q + \tilde{q})$ . In this case, we consider the dynamical equations for the ratios of zonal energy and fluctuation energy

$$\frac{\tilde{E}(t)}{E(t)} + \frac{\bar{E}(t)}{E(t)} = 1,$$

with  $\tilde{E} = \frac{1}{2} \left( \|\nabla\tilde{\varphi}\|_0^2 + \|\tilde{\varphi}\|_0^2 \right)$  the energy in the fluctuation and  $\bar{E} = \frac{1}{2} \|\partial_x\bar{\varphi}\|_0^2$  the energy in the zonal state. First, we have the dynamics for the total energy  $E$  and the energy in the fluctuation  $\tilde{E}$  for this damping form from (2.7)

$$\begin{aligned} \frac{dE}{dt} &= -D_2 \left( \|\Delta\varphi\|_0^2 + 2\|\nabla\tilde{\varphi}\|_0^2 + \|\tilde{\varphi}\|_0^2 \right), \\ \frac{d\tilde{E}}{dt} - (\partial_x\bar{v}, \bar{u}\bar{v})_0 &= -D_2 \left( \|\Delta\tilde{\varphi}\|_0^2 + 2\|\nabla\tilde{\varphi}\|_0^2 + \|\tilde{\varphi}\|_0^2 \right). \end{aligned}$$

Notice that there is the interaction term  $(\partial_x\bar{v}, \bar{u}\bar{v})$  between the mean and fluctuation due to the nonlinear interaction in the mean energy equation. Then we can find the dynamical equation for the ratio  $\tilde{E}/E$  through the above two equations

$$\begin{aligned} \frac{d}{dt} \left( \frac{\tilde{E}}{E} \right) &= \frac{1}{E^2} \left( \dot{\tilde{E}}E - \tilde{E}\dot{E} \right) \\ &= \frac{1}{E} (\partial_x\bar{v}, \bar{u}\bar{v})_0 \\ &\quad - \frac{D_2}{2E^2} \left[ \left( \|\Delta\tilde{\varphi}\|_0^2 + 2\|\nabla\tilde{\varphi}\|_0^2 + \|\tilde{\varphi}\|_0^2 \right) \left( \|\nabla\tilde{\varphi}\|_0^2 + \|\tilde{\varphi}\|_0^2 + \|\partial_x\bar{\varphi}\|_0^2 \right) \right. \\ &\quad \left. - \left( \|\Delta\varphi\|_0^2 + 2\|\nabla\tilde{\varphi}\|_0^2 + \|\tilde{\varphi}\|_0^2 \right) \left( \|\nabla\tilde{\varphi}\|_0^2 + \|\tilde{\varphi}\|_0^2 \right) \right] \\ &= \frac{1}{E} (\partial_x\bar{v}, \bar{u}\bar{v})_0 - \frac{D_2}{2E^2} \left( W \|\partial_x\bar{\varphi}\|_0^2 - E \|\partial_x^2\bar{\varphi}\|_0^2 \right) \\ &= \frac{1}{E} (\partial_x\bar{v}, \bar{u}\bar{v})_0 - \frac{D_2}{2E} \left( \Lambda \|\partial_x\bar{\varphi}\|_0^2 - \|\partial_x^2\bar{\varphi}\|_0^2 \right) \\ &= \frac{1}{E} (\partial_x\bar{v}, \bar{u}\bar{v})_0 - \frac{D_2}{E} \left( \Lambda (E - \tilde{E}) - (W - \tilde{W}) \right) \\ &= \frac{1}{E} (\partial_x\bar{v}, \bar{u}\bar{v})_0 + \frac{D_2}{E} \left( \Lambda\tilde{E} - \tilde{W} \right) \\ &\leq \frac{1}{E} (\partial_x\bar{v}, \bar{u}\bar{v})_0 - D_2 (1 + \Lambda_1 - \Lambda(t)) \frac{\tilde{E}}{E}. \end{aligned}$$

Above we use the relations  $\frac{W}{E} = \Lambda(t)$  and  $\tilde{W} \geq (1 + \Lambda_1)\tilde{E}$ . On the other hand, we have the estimation for the nonlinear interaction term

$$\frac{1}{E} |(\partial_x^2\bar{\varphi}, \bar{u}\bar{v})_0| \leq \frac{1}{2E} \int |\partial_x^2\bar{\varphi}| (\tilde{u}^2 + \tilde{v}^2) \leq \frac{1}{2E} \|\partial_x^2\bar{\varphi}\|_\infty \|\nabla\tilde{\varphi}\|_0^2.$$

With the selective decay principle satisfied with the the eigenvalue  $\Lambda_*$ , we can find that the upper bounds for the total energy and enstrophy decay to zero

$$\begin{aligned} \|\nabla\varphi\|_0 &\leq \|\nabla\varphi(0)\|_0 e^{-D\Lambda_*t}, \\ \|\zeta\|_0 &\leq \|\zeta(0)\|_0 e^{-D\Lambda_*t}. \end{aligned}$$

Assuming the solution  $\bar{\varphi}$  is smooth on a bounded domain, then it implies that the maximum value of zonal vorticity is bounded by any small value,  $\|\partial_x^2\bar{\varphi}\|_\infty \leq c$ , as time goes on. Therefore for any small value  $\epsilon > 0$ , after large enough time  $t > T$ , the nonlinear interaction term can always be controlled

$$\frac{1}{E} |(\partial_x^2\bar{\varphi}, \bar{u}\bar{v})_0| \leq \frac{c}{2E} \|\nabla\tilde{\varphi}\|_0^2 = \epsilon \frac{\tilde{E}}{E}.$$

The second term in the dynamics of  $\Lambda(t)$  then becomes negative when  $1 + \Lambda_1 > \Lambda(t)$  at some point of the time, and is guaranteed in later times due to the monotonicity of  $\Lambda(t)$ . Thus the ratio  $\tilde{E}/E$  is always decreasing in time after the quotient  $\Lambda(t)$  reaches the value below  $\Lambda_1 + 1$ .

Notice that we achieve the above result based on the special damping form  $-D_2(-\Delta q + \tilde{q})$ , thus it is less general than the previous argument that can include an additional anti-damping operator as a forcing effect. Still it offers a rigorous proof for the decay of the fluctuation mode and the final convergence to the zonal structure shown in the numerical results.

## References

- [1] Robert L Dewar and Raden Farzand Abdullatif. Zonal flow generation by modulational instability. In *Frontiers in Turbulence and Coherent Structures*, pages 415–430. World Scientific, 2007.
- [2] Patrick H Diamond, SI Itoh, K Itoh, and TS Hahm. Zonal flows in plasma—a review. *Plasma Physics and Controlled Fusion*, 47(5):R35, 2005.
- [3] W Dorland and GW Hammett. Gyrofluid turbulence models with kinetic effects. *Physics of Fluids B: Plasma Physics*, 5(3):812–835, 1993.
- [4] W Dorland, GW Hammett, Liu Chen, W Park, SC Cowley, S Hamaguchi, and W Horton. Numerical simulations of nonlinear 3-d itg fluid turbulence with an improved landau damping model. *Bull. Am. Phys. Soc.*, 35:2005, 1990.
- [5] C Foias and JC Saut. Asymptotic behavior, as  $t \rightarrow \infty$  of solutions of navier–stokes equations and nonlinear spectral manifolds. *Indiana University mathematics journal*, 33(3):459–477, 1984.
- [6] Akira Hasegawa and Kunioki Mima. Pseudo-three-dimensional turbulence in magnetized nonuniform plasma. *The Physics of Fluids*, 21(1):87–92, 1978.
- [7] W Horton. Drift waves and transport. *Reviews of Modern Physics*, 71(3):735, 1999.
- [8] Andrew J Majda. *Introduction to turbulent dynamical systems in complex systems*. Springer, 2016.
- [9] Andrew J Majda and Margaret Holen. Dissipation, topography, and statistical theories for large-scale coherent structure. *Communications on Pure and Applied Mathematics: A Journal Issued by the Courant Institute of Mathematical Sciences*, 50(12):1183–1234, 1997.
- [10] Andrew J. Majda and Di Qi. Strategies for reduced-order models for predicting the statistical responses and uncertainty quantification in complex turbulent dynamical systems. *SIAM Review*, in press, 60(3), 2018.
- [11] Andrew J Majda, Di Qi, and Antoine J Cerfon. A flux-balanced fluid model for collisional plasma edge turbulence: Part i. model derivation and basic physical features. *arXiv preprint arXiv:1807.08054*, 2018.
- [12] Andrew J Majda, Sang-Yeun Shim, and Xiaoming Wang. Selective decay for geophysical flows. *Methods and applications of analysis*, 7(3):511–554, 2000.
- [13] Andrew J Majda and Xiaoming Wang. *Nonlinear dynamics and statistical theories for basic geophysical flows*. Cambridge University Press, 2006.
- [14] WH Matthaeus, WT Stribling, D Martinez, S Oughton, and D Montgomery. Decaying, two-dimensional, Navier-Stokes turbulence at very long times. *Physica D: Nonlinear Phenomena*, 51(1-3):531–538, 1991.
- [15] David Montgomery, Xiaowen Shan, and William H Matthaeus. Navier–stokes relaxation to sinh–poisson states at finite reynolds numbers. *Physics of Fluids A: Fluid Dynamics*, 5(9):2207–2216, 1993.
- [16] Ryusuke Numata, Rowena Ball, and Robert L. Dewar. Bifurcation in electrostatic resistive drift wave turbulence. *Physics of Plasmas*, 14(10):102312, 2007.
- [17] Joseph Pedlosky. *Geophysical fluid dynamics*. Springer Science & Business Media, 2013.
- [18] Andrey V Pushkarev, Wouter JT Bos, and Sergey V Nazarenko. Zonal flow generation and its feedback on turbulence production in drift wave turbulence. *Physics of Plasmas*, 20(4):042304, 2013.
- [19] Di Qi and Andrew J. Majda. Low-dimensional reduced-order models for statistical response and uncertainty quantification: Two-layer baroclinic turbulence. *Journal of the Atmospheric Sciences*, 73(12):4609–4639, 2016.
- [20] Di Qi, Andrew J Majda, and Antoine Cerfon. A flux-balanced model for collisional plasma edge turbulence: Part II. numerical simulations with different aspect ratios. *in preparation*, 2018.

- [21] Peter B Rhines. Waves and turbulence on a beta-plane. *Journal of Fluid Mechanics*, 69(3):417–443, 1975.
- [22] Rick Salmon. *Lectures on geophysical fluid dynamics*. Oxford University Press, 1998.
- [23] Masahiro Wakatani and Akira Hasegawa. A collisional drift wave description of plasma edge turbulence. *The Physics of fluids*, 27(3):611–618, 1984.
- [24] Hongxuan Zhu, Yao Zhou, and IY Dodin. On the rayleigh–kuo criterion for the tertiary instability of zonal flows. *arXiv preprint arXiv:1805.02233*, 2018.